



You have downloaded a document from
RE-BUS
repository of the University of Silesia in Katowice

Title: Spatio-temporal localization of selected pectic and arabinogalactan protein epitopes and the ultrastructural characteristics of explant cells that accompany the changes in the cell fate during somatic embryogenesis in *Arabidopsis thaliana*

Author: Izabela Potocka, Kamila Godel, Izabela Dobrowolska, Ewa U. Kurczyńska

Citation style: Potocka Izabela, Godel Kamila, Dobrowolska Izabela, Kurczyńska Ewa U. (2018). Spatio-temporal localization of selected pectic and arabinogalactan protein epitopes and the ultrastructural characteristics of explant cells that accompany the changes in the cell fate during somatic embryogenesis in *Arabidopsis thaliana*. "Plant Physiology and Biochemistry" (Vol. 127 (2018), s. 573-589), doi 10.1016/j.plaphy.2018.04.032



Uznanie autorstwa - Użycie niekomercyjne - Bez utworów zależnych Polska - Licencja ta zezwala na rozpowszechnianie, przedstawianie i wykonywanie utworu jedynie w celach niekomercyjnych oraz pod warunkiem zachowania go w oryginalnej postaci (nie tworzenia utworów zależnych).



UNIWERSYTET ŚLĄSKI
W KATOWICACH



Biblioteka
Uniwersytetu Śląskiego



Ministerstwo Nauki
i Szkolnictwa Wyższego



Research article

Spatio-temporal localization of selected pectic and arabinogalactan protein epitopes and the ultrastructural characteristics of explant cells that accompany the changes in the cell fate during somatic embryogenesis in *Arabidopsis thaliana*

Izabela Potocka, Kamila Godel, Izabela Dobrowolska, Ewa U. Kurczyńska*

Department of Cell Biology, Faculty of Biology and Environmental Protection, University of Silesia, Jagiellońska 28, 40-032, Katowice, Poland

ARTICLE INFO

Keywords:

Arabidopsis thaliana, arabinogalactan proteins
Pectins
Pluripotent
Somatic embryogenesis
Totipotent
Ultrastructure

ABSTRACT

During somatic embryogenesis (SE), explant cells undergo changes in the direction of their differentiation, which lead to diverse cell phenotypes. Although the genetic bases of the SE have been extensively studied in *Arabidopsis thaliana*, little is known about the chemical characteristics of the wall of the explant cells, which undergo changes in the direction of differentiation. Thus, we examined the occurrence of selected pectic and AGP epitopes in explant cells that display different phenotypes during SE. Explant examinations have been supplemented with an analysis of the ultrastructure. The deposition of selected pectic and AGP epitopes in somatic embryos was determined.

Compared to an explant at the initial stage, a/embryogenic/totipotent and meristematic/pluripotent cells were characterized by a decrease in the presence of AGP epitopes, b/the presence of AGP epitopes in differentiated cells was similar, and c/an increase of analyzed epitopes was detected in the callus cells. Totipotent cells could be distinguished from pluripotent cells by: 1/the presence of the LM2 epitope in the latest one, 2/the appearance of the JIM16 epitope in totipotent cells, and 3/the more abundant presence of the JIM7 epitope in the totipotent cells. The LM5 epitope characterized the wall of the cells that were localized within the mass of embryogenic domain. The JIM8, JIM13 and JIM16 AGP epitopes appeared to be the most specific for the callus cells.

The results indicate a relationship between the developmental state of the explant cells and the chemical composition of the cell walls.

1. Introduction

The ability of somatic plant cells to change their developmental fate and to regenerate new tissues, organs and the whole plant body is a widely known phenomenon (Fehér et al., 2003; Verdeil et al., 2007). The switch from a somatic to a totipotent or pluripotent cell state involves cellular reprogramming, including (among others) chromatin reorganization, changes in the gene expression patterns and in the cell wall composition and architecture (Fowler et al., 1998; Namasivayam et al., 2006; Fehér, 2015). However, the mechanisms that underlie these processes are still not fully recognized and understood despite the large amount of research and multidisciplinary approaches in the field (for a review see Fehér, 2015).

The primary cell walls play important and diverse roles in

regulating the morphogenetic processes (Knox, 1992). The peculiar chemical composition of the cell wall is thought to be crucial for establishing and/or maintaining the cellular differentiation status (Ikeuchi et al., 2013; Corral-Martinez et al., 2016). Among the numerous cell wall polysaccharides, pectins are the most structurally complex class of macromolecules. They participate in cell expansion and adhesion and are key determinants of the physical properties of the cell wall (Willats et al., 2001). It is well established that SE is accompanied by modifications of the structure and molecular composition of the cell wall (Kikuchi et al., 1995; Smertenko and Bozhkov, 2014; Rosas et al., 2016). Studies concerning the SE of different species have revealed changes in the presence of different pectic epitopes as well as the degree of the methyl-esterification of pectic homogalacturonan during the acquisition of embryogenic competence and the development of

Abbreviations: Pd, plasmodesmata; RAM, root apical meristem; SE, somatic embryogenesis; SAM, shoot apical meristem

* Corresponding author.

E-mail address: ewa.kurczynska@us.edu.pl (E.U. Kurczyńska).

<https://doi.org/10.1016/j.plaphy.2018.04.032>

Received 27 March 2018; Received in revised form 24 April 2018; Accepted 24 April 2018

Available online 26 April 2018

0981-9428/© 2018 The Authors. Published by Elsevier Masson SAS. This is an open access article under the CC BY-NC-ND license (<http://creativecommons.org/licenses/by-nc-nd/4.0/>).

somatic embryos (Verdeil et al., 2007; Xu et al., 2011; Rodríguez-Sanz et al., 2014; Rocha et al., 2016). Despite the large number of studies reporting changes in the pectic epitopes during SE, information concerning Arabidopsis is still limited, especially within the explant, where the cells that follow different developmental programs are adjacent.

The second important chemical component of the cell wall are the arabinogalactan proteins (AGPs; e.g. Seifert and Roberts, 2007). The use of monoclonal antibodies and Yariv reagents has demonstrated the involvement of AGPs in various cellular and developmental processes such as cell division and expansion (Langan and Nothnagel, 1997), programmed cell death (Chaves et al., 2002), vascular differentiation and pattern formation (Dolan et al., 1995), sexual reproduction (Qin and Zhao, 2006) and SE (e.g. Rajesh et al., 2016). The results of the above-mentioned studies show that AGPs are important components of the signaling system and are also convenient markers for studying the developmental fate of cells (Schultz et al., 1998). It was shown that the outer cell wall surface of embryogenic cells contains arabinogalactan proteins, which are so specific that they can be used as markers of embryogenic cell clusters (Rumyantseva et al., 2003). It is also known that some AGPs can stimulate or inhibit SE (McCabe et al., 1997; Thompson and Knox, 1998). Despite numerous data indicating the involvement of AGPs in the SE process on different structural levels, including their distribution within the cell wall of somatic embryos (for review see Smertenko and Bozhkov, 2014), the distribution of AGPs within the explant cells that realize different developmental programs in the model plant Arabidopsis remain poorly described.

The above mentioned role of pectin and AGPs in the different developmental processes indicate that changes in the chemical composition of the walls may be a good marker of changes in the direction of cell differentiation during the SE process. It was shown that the main biological processes that are activated in response to SE-inductive treatment were mainly related, among others, to cell wall remodeling (Mozgová et al., 2017). In the model plant, *Arabidopsis thaliana*, the major pathways of *in vitro* morphogenesis are relatively well described on the histological, genetic and molecular levels (Gaj et al., 2005; Kurczyńska et al., 2007; Wójcikowska and Gaj, 2017). Knowledge about changes in the cell wall composition during Arabidopsis SE is rather scarce and refers to the expression of a glycine-rich gene (*Atgrp-5*) in the embryogenic callus and in the somatic embryos (Magioli et al., 2001), the distribution of lipid transfer proteins in explant cells during the induction of SE (Potocka et al., 2012) and the distribution of some pectic epitopes in the somatic embryos (Sala et al., 2013). As was pointed by Fehér (2015), the orderly deposition of structural cell wall materials such as cellulose, hemicellulose and pectin is critical for establishing and/or maintaining the cellular differentiation status. Thus, analysis of spatio-temporal changes in explant cells is worth studying.

The ultrastructural characteristics of cells that display different phenotypes within the explant during SE is also not well known. The most cited characteristics of pluripotent cells are the high nucleus/cytoplasm ratio, an isodiametric cell shape, a spherically shaped nucleus with one or more nucleoli, small vacuoles and a thin cell wall that is traversed by plasmodesmata (for review see Verdeil et al., 2007). In the case of the totipotent cells that originate from the somatic cells, the typical ultrastructure consists of a large, centrally positioned nucleus with a prominent nucleolus that is surrounded by starch and a high nucleus/cytoplasm ratio (for review see Verdeil et al., 2007). A detailed description of the ultrastructure of the cells in an Arabidopsis explant during direct SE has not yet been provided.

The literature data primarily relate to the characteristics of the ECM (extracellular matrix) within the embryogenic masses, and rarely provide information on the individual cells within them. Even less information exists about the correlation between the chemical composition of the cell walls and the totipotent/pluripotent cells. Despite many studies, the presence of different pectic and AGP epitopes within the walls of explant cells is not known. Furthermore, it is not known whether the embryogenic/totipotent cells differ in their cell wall

composition from the meristematic/pluripotent cells and/or other explant cells, which do not undergo changes in their direction of differentiation. Thus, the aim of the study was to answer the question whether the changes in the fate of explant cells during Arabidopsis SE are related to changes in the chemical composition of the cell walls. Verification of this hypothesis will permit the identification of the cells that follow the embryogenic/totipotent, non-embryogenic and pluripotent/meristematic pathways in terms of the distribution of the pectic and AGP epitopes on a histological level. In addition, the distribution of pectic and AGP epitopes in somatic embryos and the ultrastructure of explant cells were also analyzed.

2. Materials and methods

2.1. Plant material and culture conditions

Immature zygotic embryos of *Arabidopsis thaliana* L. Heynh. (ecotype Col-0) were used as explants to induce SE according to the method described by Gaj (2001). Embryos at the late cotyledonary stage of development were excised from the siliques and grown on a Phytigel-solidified (Sigma, Poland) (3.5 g L^{-1}) B5 medium (Sigma, Poland) (Gamborg et al., 1968), which had been supplemented with $5 \mu\text{M}$ 2,4-dichlorophenoxyacetic acid and 20 g L^{-1} sucrose (pH 5.8). The cultures were kept at 23°C under a 16 h photoperiod with a light intensity of $40 \mu\text{mol m}^{-2} \text{ s}^{-1}$ for three weeks.

2.2. Sample preparation

Twenty to thirty explants were collected at various time points during the culture period (days 0, 1, 3, 5, 7, 10, 14 and 21) and fixed in a mixture of 4% formaldehyde, 1% glutaraldehyde, 0.1% Triton X-100, 2 mM CaCl_2 and 1% sucrose in phosphate-buffered saline (PBS; 137 mM NaCl, 2.7 mM KCl, 10 mM Na_2HPO_4 , 1.8 mM KH_2PO_4) at pH 7.2 for 24 h at 4°C . The samples were then washed in PBS (pH 7.2), dehydrated in a graded ethanol series and infiltrated in LR White resin (medium grade, Polysciences, Germany) according to the following schedule: 3:1, 1:1, 1:3 (v/v) ethanol/LR White, each step for 24 h and 100% LR White for 36 h with a change of resin every 12 h. Finally, the material was embedded in gelatine capsules with fresh LR White resin and polymerized for 8 h at 50°C . Semi-thin sections ($0.5\text{--}1 \mu\text{m}$) were cut using a Leica EM UC6 ultramicrotome (Leica Microsystems, Germany) and mounted on poly-L-lysine coated microscope slides (Menzel-Glaser, Germany).

2.3. Histochemical staining

To demonstrate the general cytological features of the explant cells, the LR White sections were stained with 0.1% toluidine blue O (Sigma, Poland) in PBS. For the localization of proteins, the sections were stained with 1% naphthol blue black (NBB, Sigma-Aldrich, Poland) in 7% acetic acid for 10 min at $50\text{--}60^\circ\text{C}$ (Fisher, 1968). The cell wall polysaccharides and starch were visualized using the periodic acid-Schiff's (PAS) reaction. For nuclei visualization, the sections were stained with DAPI. Microscopic observations were performed using an Olympus BX41 microscope equipped with an Olympus XC50 camera (Olympus, Poland).

2.4. Monoclonal antibodies and immunofluorescence labeling

Sections were blocked in 2% fetal bovine serum (Sigma, Poland) and 2% bovine serum albumin (Jackson ImmunoResearch Laboratories, UK) in PBS for 30 min to mask any non-specific binding sites and then incubated with primary monoclonal antibodies diluted 1:10 in the above described solution at 4°C overnight. All of the primary antibodies used in the study were purchased from PlantProbes (Leeds, UK) and are listed in Table 1. After washing in the blocking buffer ($5 \times 10 \text{ min}$), the

Table 1
Primary antibodies used in the study.

Antibody	Epitope	References
Anti-pectin		
JIM5	Low methyl-esterified HG	Clausen et al. (2003)
JIM7	Highly methyl-esterified HG	Clausen et al. (2003)
LM5	(1→4)-β-D-galactan	Jones et al. (1997)
Anti-AGP		
LM2	β-D-GlcpA	Smallwood et al. (1996), Yates et al. (1996)
JIM4	β-D-GlcpA-(1→3)-α-D-GalpA-(1→2)-L-Rha	Knox et al. (1989), Yates et al. (1996)
JIM8	AGP glycan	McCabe et al. (1997), Pennell et al. (1991)
JIM13	β-D-GlcpA-(1→3)-α-D-GalpA-(1→2)-L-Rha	Knox et al. (1991), Yates et al. (1996)
JIM16	AGP glycan	Knox et al. (1991), Yates et al. (1996)

sections were incubated with the secondary antibody (Alexa Fluor 488-conjugated AffiniPure goat anti-rat IgG H + L, Jackson ImmunoResearch Laboratories, UK) diluted 1:100 in the same buffer for 1 h at room temperature. Finally, the slides were washed in the blocking buffer (5 × 10 min), rinsed in PBS followed by sterile distilled water and mounted with a Fluoromount aqueous mounting medium (Sigma, Poland). The sections were examined using an Olympus BX41 epifluorescence microscope (excitation filter BP470-490, dichromatic mirror DM500, barrier filter BA520IF). Images were captured using an Olympus XC50 camera. To reveal the cellular pattern, immunolabeled sections were viewed and photographed using phase contrast optics.

For each developmental stage (day of culture), at least 5 samples were probed with each of the above mentioned monoclonal antibodies. Control reactions were performed by omitting the primary antibody from the procedure and by incubating the sections with the blocking buffer solution. They did not show any labeling except for a faint background autofluorescence (data not shown).

The intensity of the immunolabeling was evaluated according to Pielach et al. (2014). The following types of cells within the explants were taken into consideration: the embryogenic cells of the protoderm and/or subprotoderm, the meristematic cells of the protoderm and/or subprotoderm, the highly vacuolated cells of the ground tissue – here termed “differentiated cells” and the callus cells (Table 2).

2.5. Transmission electron microscopy (TEM)

Samples from the explants were collected at various time points during the culture period (days 0, 3, 7, 14) and were fixed in 2.5% glutaraldehyde and 2.5% paraformaldehyde in a 0.05 M cacodylate buffer (Sigma; pH 7.2) and kept for 24 h at 4 °C. Next, they were washed in the buffer, postfixed in 1% osmium tetroxide (Serva, Heidelberg, Germany) in distilled water at 4 °C overnight, dehydrated in a graded series of ethanol and gradually embedded in Epon resin (Polysciences, Germany) according to method described earlier (Milewska-Hendel et al., 2017). For the TEM analysis, ultrathin sections, 70 nm thick, were obtained using a Leica EM UC6 ultramicrotome and were collected on copper grids (300 mesh, Electron Microscopy Science, Hatfield, PA, USA). Grids with sections were stained with a saturated solution of uranyl acetate (Polysciences, Germany) in 50% ethanol for 15 min and 0.04% lead citrate agents (Sigma, Poland) for 10 min. The sections were examined using a Hitachi H500 electron microscope (Hitachi, Tokyo, Japan) at 75 kV in the Faculty of Biology and Environmental Protection, University of Silesia in Katowice.

3. Results

Morphological changes of the explants primarily concerned the

straightening of the cotyledons, the swelling of the cotyledon node and the development of somatic embryos (Fig. 1A–D). At the initial stage of the culture, the explants (immature zygotic embryo – IZE) were characterized by bent cotyledons (Fig. 1A). The first morphological change of the IZEs was the straightening of the cotyledons and the swelling of their proximal adaxial sides (Fig. 1B). During the following days, somatic embryos at the early stages of development were visible (Fig. 1C). Mature somatic embryos were present on the explants between 14 and 21 days of the culture (Fig. 1D).

3.1. Characteristics of the explant cells at the initial stage of the culture

The overall description of the occurrence of pectic and AGP epitopes in different cell phenotypes of the explants during the culture is presented in Table 2. Below, we describe our results in detail.

The initial explant (IZE) was composed of meristematic pluripotent cells that were located in the shoot and root apical meristem (SAM and RAM, respectively), the protoderm, ground meristem and provascular tissue (Fig. 2A). The meristematic cells in the SAM were characterized by a spherically shaped nucleus with one or two (generally small) nucleoli, a fragmented vacuole, dense cytoplasm and a lack of amyloplasts (Fig. 2A, inset, 2B; cells with the above mentioned features have been further considered to be meristematic/pluripotent regardless of their localization in the explants and the time of the culture). The protodermal and ground meristem cells contained many small vacuoles, numerous protein bodies and plastids with starch grains (Fig. 2A and B). The provascular cells were characterized by small starch granules and elongated nuclei (Fig. 2A and B).

At the initial stage of the culture, the pectic epitope that was recognized by the JIM5 antibody occurred in the walls of each explant cell (Fig. 2C). In the protodermal cells, the JIM5 epitope was present mostly in the cell corners between the anticlinal and outer periclinal cell walls (PEG) of the protoderm (Fig. 2C, arrowheads; Table 2). The JIM7 epitope was detected within the walls of the explant cells and a lower presence of this epitope characterized the protodermal cells of the explants (Fig. 2D). The most pronounced differences between the distribution of the JIM5 and JIM7 pectic epitopes concerned the protodermis – the JIM7 epitope was not present in the outer periclinal walls except for the PEG areas (Table 2). The LM5 epitope was abundantly present in all of the explant cells (Fig. 2E; Table 2). Immunolabeling with anti-AGP antibodies revealed the abundant presence of the LM2 epitope in all of the explant cells, in both cell walls and intracellular compartments (Fig. 2F; Table 2). The JIM8 and JIM13 epitopes were only detected in some provascular cells (Fig. 2G; Table 2). The AGP epitopes that were recognized by the JIM4 and JIM16 antibodies were not detected within the explant cells at the initial stage of the culture (not shown; Table 2).

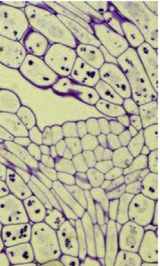
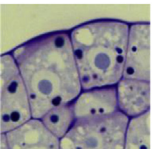
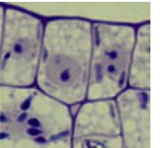
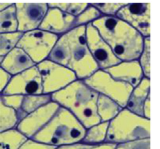
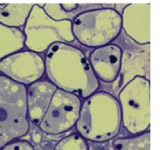
3.2. Cytological and immunocytochemical changes of the explant cells during the culture

Numerous time points were analyzed during the duration of the culture. However, the results presented here concern only those in which significant and histological changes occurred (Kurczyńska et al., 2007).

3.2.1. Pectic epitopes

After about 3 days, the intensity of the JIM5 and JIM7 labeling increased significantly in the region of the cotyledonary node of the explants. The most intensive labeling characterized the walls of the cells in the adaxial proximal parts of the cotyledons (Fig. 3A). In this region, an increased number of cell layers (compared to the initial stage of the culture) was detected and this was the result of the cell division of the explant ground promeristem. Such cells were characterized by a thin layer of cytoplasm, a prominent nucleus and one or more vacuoles (Fig. 3A', compare Figs. 2 and 3A, A'). The JIM5 pectic epitope was

Table 2
Summarised results of immunolabeling for the various types of cells in *Arabidopsis* explants.

	Pectins			Arabinogalactan proteins					
	JIM5	JIM7	LM5	JIM4	JIM8	LM2	JIM13	JIM16	
Explant at day 0									
	Protoderm								
	outer periclinal walls	±	-	++	-	-	++	-	-
	anticlinal walls	±	-	++	-	-	++	-	-
	inner periclinal walls	±	-	++	-	-	++	-	-
	PEG	++	++	++	-	-	++	-	-
	intracellular compartments	-	-	+	-	-	++	-	-
	Ground promeristem								
	Provascular tissue	±	±	±	-	-	++	-	-
	SAM	±	±	±	-	-	++	-	-
	Explant after 1 week of the culture								
	Totipotent/embryogenic cells								
	Extracellular matrix	-	++	-	-	-	-	-	±
	Cell wall	+	++	+	-	-	-	-	-
	Pluripotent/meristematic cells								
	Extracellular matrix	-	-	-	-	-	-	-	-
	Cell wall	±	±	±	-	-	+	-	-
	Differentiated cells								
	Extracellular matrix	-	-	-	-	+	-	-	-
	Cell wall	+	+	±	+	+	±	-	-
	Callus cells								
	Extracellular matrix	++	-	-	-	-	++	-	++
	Cell wall	++	++	++	-	++	++	+	++
Intracellular compartments	++	+	++	++	+	++	±	++	

The intensity of labeling was evaluated as - no labeling, ± weak labeling, + moderate labeling and ++ strong labeling (because it is difficult to identify the separate fluorescence signals in the cell wall and plasma membrane at the light microscopy level, in the case of the AGP epitopes, the two compartments are described together; signals inside the cells were classified as being localized in the intracellular compartments or in short in the cytoplasm; see Results).

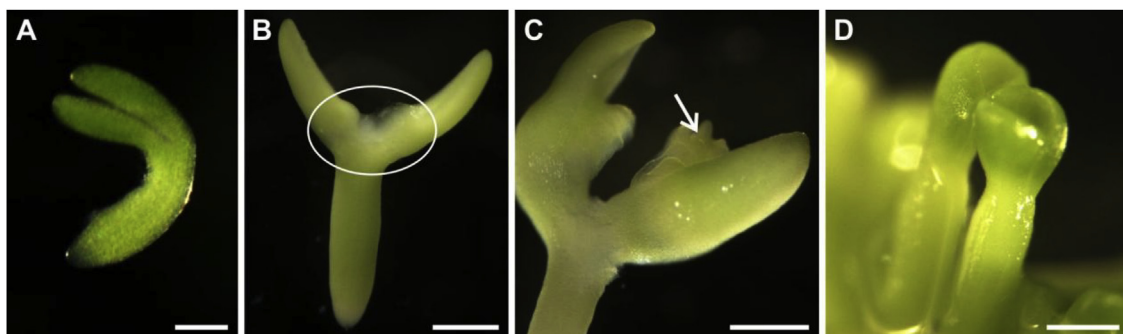


Fig. 1. Morphology of the *Arabidopsis thaliana* explants during the *in vitro* culture. (A) Initial explant with bent cotyledons. (B) Between 5 and 7 days of the culture, the swelling of the cotyledon node (ellipse) occurred. (C) In the 2nd week of the culture, somatic embryos were present in the proximal, adaxial part of the cotyledons (arrow). (D) After 3 weeks of culture, well-developed somatic embryos cover the whole explant. Scale bars: (A-C) = 200 µm, (D) = 500 µm.

almost not detected in the walls of the abaxial protodermis and one layer of the abaxial ground promeristem (Fig. 3A). Although the pattern of JIM7 labeling was the same as JIM5, the anticlinal walls of the adaxial/abaxial protodermis and subprotodermal cells of the abaxial

side of the explant cotyledon were only slightly labeled (Fig. 3B).

The patterns of labeling with the JIM5 antibody remained unchanged on day 5 and later, but the JIM7 epitope was temporally absent in the hypocotyl part of the cotyledonary node (Fig. 3C and D) and it

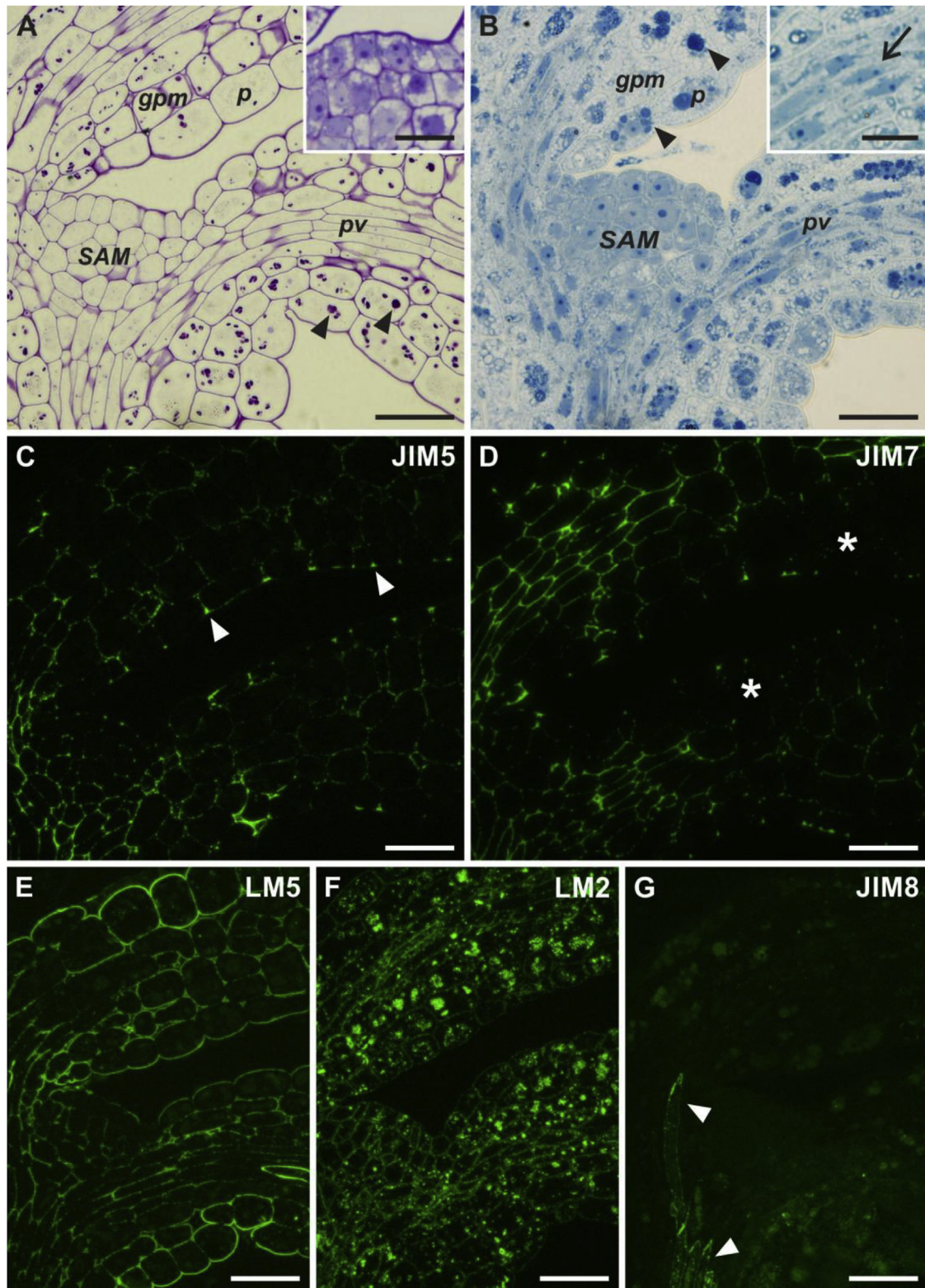


Fig. 2. Longitudinal sections of the explants at the initial stage (day 0) in the region of the cotyledonary node. (A) PAS and TBO staining, cell wall polysaccharides and starch (arrowheads) are stained purplish red; inset: a magnified view of the meristematic cells in the SAM. (B) NBB staining, protein-containing bodies (arrowheads) stained blue; inset: a magnified view of the provascular cells (arrow points to the elongated nucleus). (C) Immunodetection of pectins with the JIM5 antibody, strongly labeled junctions between the protodermal cell walls (arrowheads). (D) Immunodetection of pectins with the JIM7 antibody, weak labeling in the protodermal and subprotodermal cells (asterisks). (E) Immunodetection of pectins with the LM5 antibody, strong labeling in the cell walls of the explants. (F) Immunodetection of AGPs with the LM2 antibody, strong punctate signals in the cell wall/plasma membrane and in the cytoplasm compartments. (G) Immunodetection of AGPs with the JIM8 antibody, strong labeling in the provascular cells (arrowheads). SAM, shoot apical meristem; p, protoderm; gpm, ground promeristem; pv, provascular tissue. Scale bars: (A, B, insets) = 10 μ m, (A–G) = 20 μ m. (For interpretation of the references to color in this figure legend, the reader is referred to the Web version of this article.)

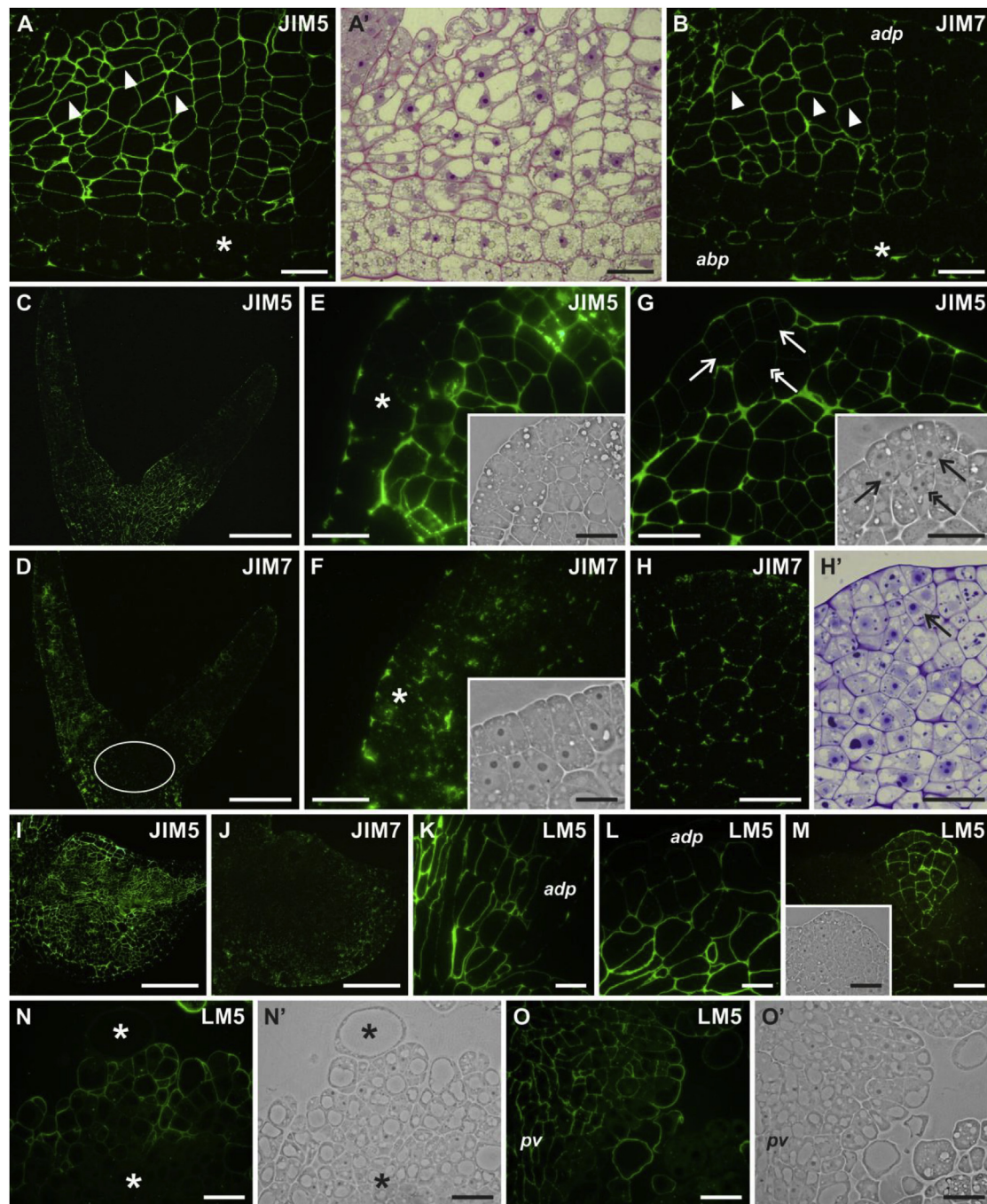


Fig. 3. Immunofluorescent detection of the pectic epitopes in the *Arabidopsis* explants. (A–J) Labeling with the JIM5 and JIM7 antibodies. (A, B) Magnified views of the proximal parts of the cotyledons, day 3 of the culture, the strongest signal in the cell walls in the adaxial part of the cotyledon (arrowheads), weak labeling in the abaxial protoderm and subprotoderm layers (asterisks). (A') A consecutive section stained with TBO that shows the cytological features of the cotyledonary cells. (C, D) Distribution of the HG epitopes in the explants cultured for 5 days, the ellipse in D indicates the unlabeled area of the cotyledon node. (E, F) Elongated protoderm cells (asterisks) in the proximal parts of the cotyledons, day 7 of the culture, weak JIM5 and JIM7 labeling; insets: phase contrast views of the sections. (G, H) The presence of HG epitopes in periclinally divided protoderm cells, day 7 of the culture; inset in G: phase contrast view of the section, arrows indicate embryogenic cells, double arrow indicates the meristematic cell. (H') A consecutive section stained with TBO, arrow indicates an embryogenic cell. (I, J) Distribution of the HG epitopes in 2-week-old explant, note the clear difference in the labeling patterns. (K–O) Labeling with the LM5 antibody. (K, L) Magnified views of the proximal parts of the cotyledons, day 3 of the culture, weak labeling in the protoderm. (M) Localization of the epitope within the embryogenic protrusion, day 14 of the culture; inset: phase contrast view of the section, cell phenotypes visible. (N, O) The presence of the epitope in the surface cells of the explants cultured for 14 days, asterisks in N and N' indicate unlabeled cells. (N', O') Phase contrast views of the sections N, O. adp, adaxial protoderm; abp, abaxial protoderm; pv, provascular bundle. Scale bars: (K, L) = 10 μ m, (A–B, E–H', M–O' and E–G, M, insets) = 20 μ m, (C, D, I, J) = 100 μ m.

reappeared in this area in the subsequent days (data not shown). After the next few days in some areas of protodermis in the embryogenic part of the explants, elongating cells were detected and these cells were devoid of a JIM5 fluorescence signal primarily in the anticlinal walls

(Fig. 3E). The same was observed for the JIM7 signal (Fig. 3F). Later, the elongated cells underwent periclinal divisions, and then the signal that was generated by the JIM5 and JIM7 antibody occurred again in walls of these cells (Fig. 3G and H). Differences between the

distribution of the pectic epitopes that were recognized by JIM5 and JIM7 antibody were related to the intensity of the signal and its character (Fig. 3G and H). By the end of the 1st week, some cells in the embryogenic part of the explants displayed the phenotype of an embryogenic/totipotent character (according to Verdeil et al., 2007). They were characterized by a densely stained cytoplasm and large nuclei and prominent nucleoli (Fig. 3G, F, insets and H'). In the same part of the explants, cells with a pluripotent/meristematic phenotype were also present (Fig. 3G, inset, double arrow).

Prominent differences between the distribution of JIM5 and JIM7 signal were observed in the explant cells after about 14 days (Fig. 3I and J). The signal generated by the JIM5 antibody was abundantly present in all of the explant cells in the cotyledon node and the JIM7 signal antibody was present only at the periphery of the explants with a rather cytoplasmic localization. After 3 days of the culture, the LM5 rhamnogalacturonan-I (RG-I) epitope was detected in all of the explant cells except for the walls of the protodermis (Fig. 3K and L). After the next few days of the culture, the LM5 epitope was present within the domain of the embryogenic cells, but what was interesting was that the epitope was restricted to only some of the cells that were located within the protrusion (Fig. 3M). The signal was also observed in the cells that were located at the surface of the explants where the cells dedifferentiated into the callus (Fig. 3N, N', O, O').

3.2.2. Arabinogalactan protein epitopes

Each of the analyzed AGP epitopes exhibited a specific and different spatio-temporal distribution pattern (Figs. 4 and 5). The AGP epitope that is recognized by the JIM4 antibody appeared in the explant cells between 3 and 7 days of the culture (Fig. 4A). This epitope was present in the ground promeristem and protodermis regardless of the explant organ (Fig. 4A). Interestingly, the epitope was detected in the cytoplasmic compartments, not in the cell walls. During the next few days (about 11th day) the signal generated by the JIM4 antibody disappeared from the cytoplasm compartments in all of the explant cells and appeared in the walls of large cells with prominent one or more vacuoles (Fig. 4B). These cells were located in the vicinity of the cells lacking this epitope and that had a meristematic/pluripotent character (Fig. 4B, inset). After 2 weeks of the culture, the JIM4 epitope was present within the cytoplasmic compartments of the cells that were located near the tracheary elements (Fig. 4C, C').

The JIM8 epitope appeared in the explant cells after 5 days of the culture and was detected in the cells of the provascular bundle, perhaps in proto-phloem and xylem (Fig. 4D). After the next 3 days, the JIM8 signal occurred in all of the explant cells, mainly in the walls but also in the cytoplasmic compartments (Fig. 4E). In the 10-day-old culture, the signal was detected only in some areas of the explants (Fig. 4F). The cells revealing the JIM8 signal that was localized in the cytoplasmic compartments and cell walls were characterized by large vacuoles (Fig. 4F). In the 12-day-old culture, the signal was visible only in callus and in meristematic/pluripotent cells (Fig. 4G). After about 3 weeks the JIM8 signal was detected only in the cells that had differentiated into the tracheary elements (Fig. 4H).

The distribution of the LM2 epitope remained basically unchanged throughout the 1st week of the culture, and the same more or less uniformly scattered dotted signal was localized in the walls of the explant cells, but also in the cytoplasmic compartments with a lower intensity in the embryogenic part of the explants (not shown). In the explants that were older than 7 days, the LM2 pattern became less uniform and more cell-type dependent (Fig. 5A, A', A'', A'''). In the explant protodermal cells that had not changed their phenotype, the LM2 epitope was abundantly present in the wall/plasma membrane (this was hard to settle unless plasmolysis occurred) and the cytoplasmic compartments (Fig. 5A, A' and A'''). In the cells of the totipotent/embryogenic phenotype, a weak signal that was generated by the LM2 antibody was present only in the cell walls (Fig. 5A, A''). In the intensively dividing (pluripotent/meristematic) cells that are involved

in the formation of explant protrusions, the LM2 epitope was abundantly present (Fig. 5B, B').

The JIM13 epitope was detected in the cells of explant provascular bundle and in the cells that had differentiated into tracheary elements and in the callus (Fig. 5C). The number of cells displaying the JIM13 signal increased with the duration of the culture (Fig. 5C and inset 1). DAPI staining interacted with the JIM13 staining (Fig. 5C, inset 2).

During the 1st week of the culture, the AGP epitope that is recognized by the JIM16 antibody appeared only in the cytoplasmic compartments (Fig. 5D). Afterwards, in the following days, the JIM16 signal disappeared from the cytoplasm and was detected only in the outer periclinal walls of the protodermal cells (Fig. 5E) and/or in the middle lamella and the walls between the protodermis and sub-protodermis of the explants, but only locally (Fig. 5F). The presence of this epitope coincided with the border between the cells that are involved in the appearance of the protrusion and in the cell located beneath them (Fig. 5F inset).

3.2.3. Pectic and AGP epitopes in the callus cells

All of the analyzed pectic and AGP epitopes were detected in the callus cells (Fig. 6). The HG epitopes (JIM5, JIM7) and LM5 rhamnogalacturonan-I (RG-I) epitope were present in the cell walls (Fig. 6A–C). However, in the case of the JIM5 epitope, the presence in the plasma membrane cannot be excluded (Fig. 6A), as well as the presence of the LM5 epitope in the cytoplasmic compartments (Fig. 6C). Among the AGP epitopes, only JIM4 was not detected in the cell walls but was abundantly present in the cytoplasmic compartments (Fig. 6D). Other AGP epitopes were detected in both the cell walls and in the cytoplasmic compartments (Fig. 6E–H). The presence of the AGP epitope that is recognized by the LM2 antibody in the plasma membrane cannot be excluded (Fig. 6F). The AGP epitope that is recognized by the JIM16 antibody was also detected outside the cell wall (Fig. 6H).

3.2.4. Pectic and AGP epitope distribution in the somatic embryos at the early stages of development

Immunocytochemical detection of the pectic and AGP epitopes was also performed in the somatic embryos at the early stages of development. We selected mainly the globular and heart stage somatic embryos because these stages are easy to distinguish from other bulges on explants in cultures on a solid medium (as was shown by Dobrowolska et al., 2016, not each section with structures that resemble embryos are somatic embryos).

Among the pectic epitopes, JIM5 was more abundant in the globular somatic embryos compared to the JIM7 epitope (Fig. 7A, E). Although the same epitopes were abundant in the heart stage, the location of these epitopes varied in relation to the embryo axis; JIM5 was absent in the outer layers of the basal part and JIM7 was present in this embryo part (Fig. 7B, F; Table 3). Moreover, both epitopes were hardly present in the anticlinal walls of the protodermal cells. The pectic epitope that is recognized by the LM5 antibody in the globular stage of an embryo was detected in a few cells that were located in the apical part of the embryo (Fig. 7I) and in the heart stage in the cotyledons (Fig. 7J). The JIM4 epitope was not detected in the somatic embryos regardless of the developmental stage (Fig. 7C and D). The JIM8 epitope was occasionally detected in the cell walls of the globular embryos, but in the older stage, it was abundantly present in the embryo except for the protodermis (Fig. 7G and H). The LM2 epitope was present in the globular and heart stages, but in a much greater abundance at the younger stage (Fig. 7K and L). The JIM16 epitope was detected only in the outer periclinal walls of the protodermis regardless of the embryo stage of development (Fig. 7M and N). The AGP epitope that is recognized by the JIM13 antibody was not present in the somatic embryo except for cells that had developed into the provascular bundle (Fig. 7O).

3.2.5. Explant cells cytology and ultrastructure during the culture period

The initial explant cells were characterized by electron dense

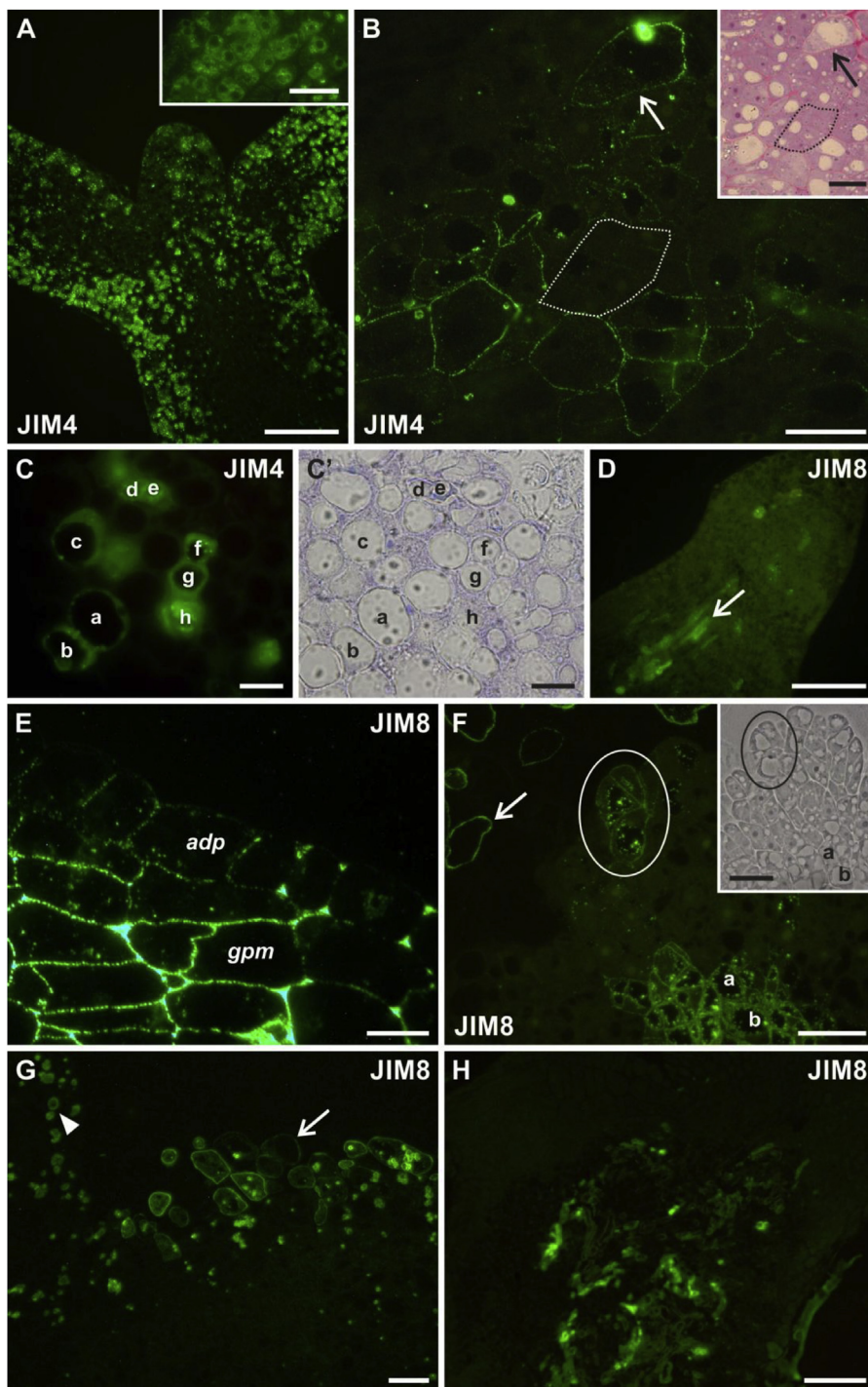


Fig. 4. Immunofluorescent detection of the AGP epitopes in the Arabidopsis explants. (A–C) Labeling with the JIM4 antibody. (A) Cytoplasmic signal in an explant cultured for 5 days; inset: details of the labeling pattern in the cotyledon cells. (B and inset) Labeling in the highly vacuolated cells of the ground promeristem (arrow), proximal part of the cotyledon of an explant cultured for 10 days, note the lack of labeling in the non-vacuolated cells (dotted line); inset: a consecutive section stained with TBO. (C) Localization of the epitope in a 2-week-old explant; (C') bright field image of the section shown in C; labeled cells are indicated by the letters a-h. (D–H) Labeling with the JIM8 antibody. (D) The presence of the epitope in the provascular tissue (arrow), day 5 of the culture. (E) Proximal part of the cotyledon of an explant cultured for 7 days, labeling in the protodermal and ground promeristem cells. (F and inset) Groups of labeled cells (ellipse, letters a and b) in an explant cultured for 10 days, arrow points to the callus cell; inset: phase-contrast view of the section, phenotypes of the labeled cells are visible. (G) Signal in the pluripotent/meristematic (arrowhead) and callus (arrow) cells, 2nd week of the culture. (H) Localization of the epitope in a three-week-old explant. adp, adaxial protoderm; gpm, ground promeristem. Scale bars: (C, C', E) = 10 μ m, (B, F, G and A, B, F, insets) = 20 μ m, (A, D, H) = 50 μ m.

cytoplasm regardless of the explant organ or tissue (Fig. 8A and B) and because they were filled with numerous oil and protein bodies with globoid crystals and starch grains, other organelles were difficult to detect (Fig. 8C). The lipid bodies were located against the plasma membrane and around the protein bodies. In the protodermal cells, a chloroplast with a system of internal membranes that were not well-developed was present (Fig. 8B, inset 1). At the initial stage in the embryonic part of explants (see Kurczyńska et al., 2007), the cell was characterized by a nucleus with one nucleolus in addition to the shoot apical meristem where two nucleoli were present in the nucleus, which indicates that only these cells are meristematic (Fig. 8A, inset). The outer periclinal cell walls of the protodermal cells were uniformly thin along the outer surface (Fig. 8B). The outer layer of the walls was

electron dense (cuticle) and the inner layer (cellulosic part of cell wall) was electron-lucent (Fig. 8B). An electron-dense layer must be composed at least in part by pectins as this layer is connected to the middle lamella between the anticlinal walls (Fig. 8B and C). Plasmodesmata (Pd) were present between all of the cells (Fig. 8B, inset 2) but in different quantities between different explant tissues.

In the subsequent days of the culture (about the 7th day), new cell phenotypes, which were determined on the basis of nucleus ultrastructure, appeared in some areas of the explants. In a close proximity, cells with a nucleus with a large prominent nucleolus, cells with two nucleoli in the nucleus and cells with a nucleus with no ultrastructural changes compared to the starting point of the culture were detected (Fig. 8D, cells that were compared are indicated by different digits;

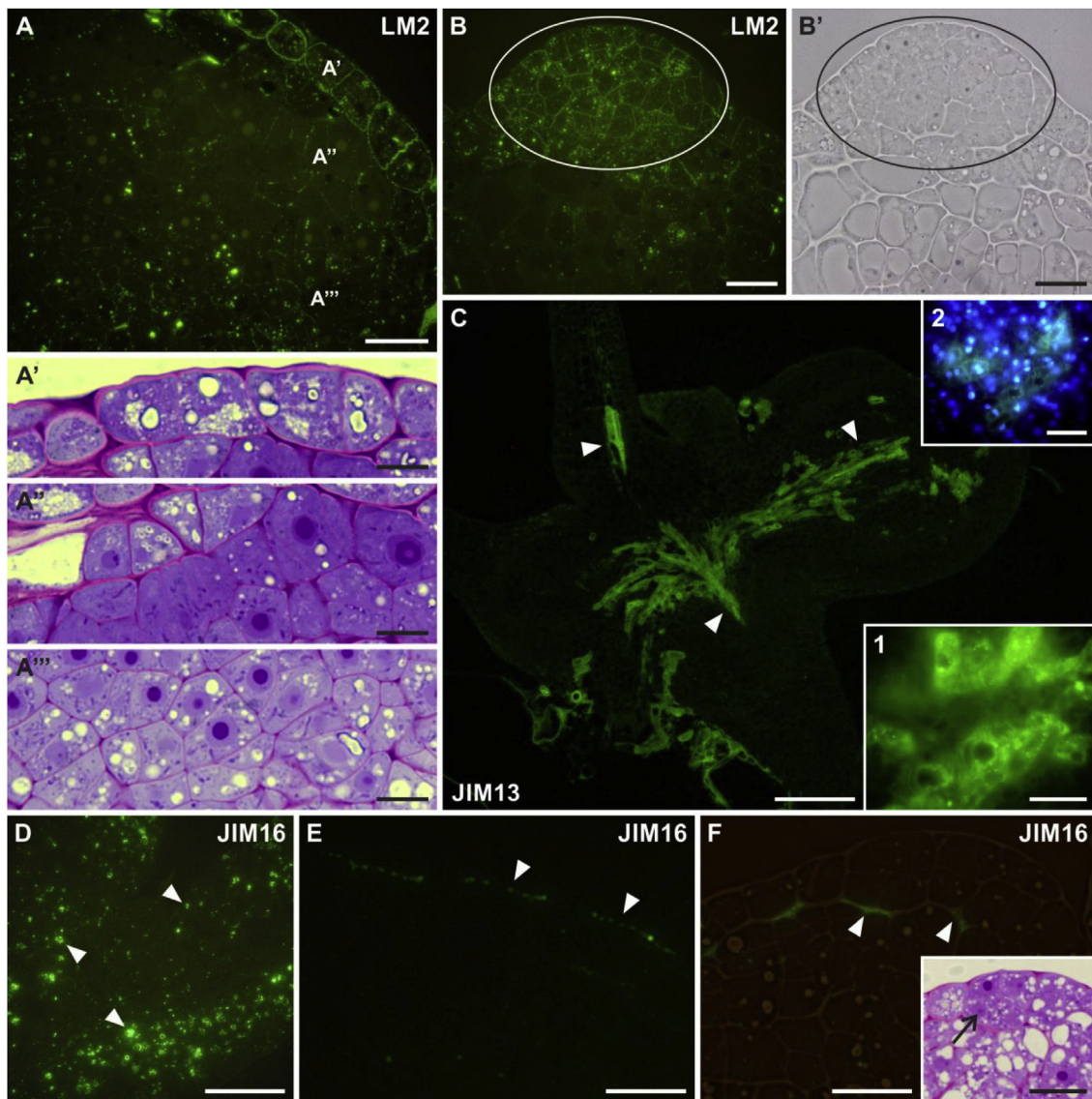


Fig. 5. Immunofluorescent detection of the AGP epitopes in the *Arabidopsis* explants. (A–B) Labeling with the LM2 antibody. (A) Distribution of the epitope in cells with diverse phenotype (marked with letters A', A'', A''') in the proximal part of the cotyledon of an explant cultured for 10 days. (A'–A''') Cytological features of the explant cells, TBO staining. (B) A group of pluripotent/meristematic cells on the surface of the cotyledon (outlined with white ellipse on B and black ellipse on B'), abundant labeling in the cell wall/plasma membrane and in the cytoplasm, no labeling in the highly vacuolated cells of the ground promeristem. (B') Phase-contrast image of the section shown in B. (C) Labeling with the JIM13 antibody, strong signal in the provascular tissue (arrowheads); insets: (1) details of the labeling pattern, (2) nuclei revealed by DAPI staining. (D–F) Labeling with the JIM16 antibody. (D) Signal in the cytoplasm of an explant cultured for 5 days (arrowheads). (E) Signal in the outer periclinal walls of the protodermal cells (arrowheads), day 7 of the culture, no labeling in the cytoplasmic compartments. (F) The presence of the epitope between the protodermal and subprotodermal cell layers (arrowheads), day 7 of the culture, merge fluorescence and bright field images; inset: a consecutive section stained with TBO, note the typical totipotent/embryogenic features (a dense cytoplasm and a single large nucleolus) of the protodermal cells (arrow). Scale bars: (A'–A''') = 10 μm , (A, B, B', E, F and C, F, insets) = 20 μm , (D) = 50 μm , (C) = 100 μm .

Fig. 8E comparison of cells number 1 and 3; **Fig. 8F** and inset, G). Such changes and changes in cell ultrastructure indicate a shift in the direction of cell differentiation (**Fig. 8E**). During this time the disappearance of the protein bodies was observed as the first sign of the ultrastructural changes within the cytoplasm (**Fig. 8E**). Cells with a nucleus with more than one nucleolus are considered to be pluripotent/meristematic and cells with a prominent nucleolus in the nucleus considered to be totipotent/embryogenic *sensu* Verdeil et al. (2007). The number of lipid bodies decreased and were no longer located close to the plasma membrane but were distributed within the cell cytoplasm, which became less electron dense (**Fig. 8E**). During this period of time, changes in the cytoplasm ultrastructure occurred, regardless of the nucleus structure and was related to the appearance of numerous mitochondria, rough endoplasmic reticulum, ribosomes, dictyosomes,

plastids and Pd (**Fig. 8I** and J). Differences in the cell wall ultrastructure appeared during these days (**Fig. 8H**). The outer electron-dense layer in some cells became thicker and undulated (**Fig. 8H** and inset 1). In the other cells, the inner part of the outer periclinal walls significantly increased in thickness (**Fig. 8H** and inset 1). Changes in the undulation and thickness of the outer periclinal wall of the protodermal cells were detected even before the disappearance of the lipid bodies (**Fig. 8H**, inset 2). The undulation of the cell walls that was detected in the cells from the embryogenic part of the explants (**Fig. 8K**) and the increase in thickness was characteristic for the cells from the non-embryogenic part of the explants (**Fig. 8L**). In the 2nd week of the culture, no further important changes in the cell ultrastructure were observed within the explants, but the abundant presence of microtubules was detected (**Fig. 8M**). The callus cells that were separated from the explants were

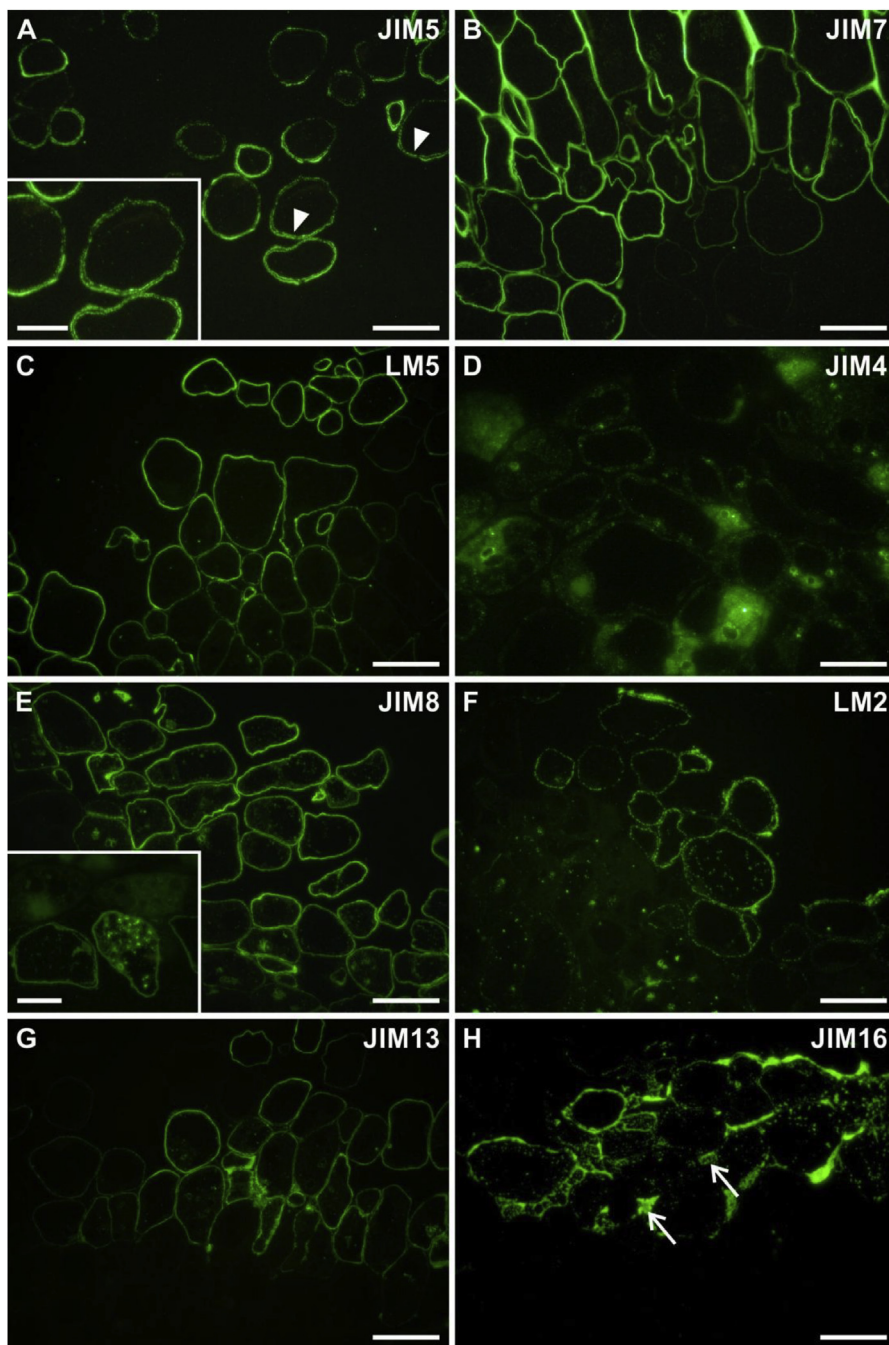


Fig. 6. Distribution of pectic and AGP epitopes within the callus tissue. (A) Labeling with the JIM5 antibody, signal in the plasma membrane face of the cell wall (arrowheads, inset). (B) Labeling with the JIM7 antibody, intense signal in the cell walls of the majority of the cells. (C) Labeling with the LM5 antibody, the epitope is present in both the cell wall and the cytoplasm. (D) JIM4 labeling in the cytoplasm. (E) JIM8 labeling in the cell wall/plasma membrane and in the cytoplasm (inset). (F) Labeling with the LM2 antibody, intense signal in the cell wall/plasma membrane and in the cytoplasm. (G) Labeling with the JIM13 antibody, strong labeling in the cell wall/plasma membrane, weak labeling in the cytoplasmic compartments. (H) Labeling with the JIM16 antibody, the abundant presence of the epitope in the intercellular spaces (arrows). Scale bars: (A, E, insets) = 10 μm , (A–H) = 20 μm .

characterized by a prominent vacuole with electron-dense particles inside, a thin layer of cytoplasm with organelles and a nucleus with a small nucleolus (Fig. 8N). The abundant presence of fibrillary material was detected in intercellular spaces during the phase of the separation of the cells from the explants (Fig. 8N, inset).

4. Discussion

The results of the present study revealed spatio-temporal changes in the distribution of the pectic and AGP epitopes in Arabidopsis explants that were committed to SE and indicated a relationship between the cell wall composition and the developmental state of the explant cells. In this paper, we describe the diverse cell wall chemical composition in the cells that are characterized by the different phenotypes that arose within the explants during the process of SE when the explant cells changed the direction of their differentiation under *in vitro* conditions.

To permit an accurate comparison among the signals from the cells that realize different developmental programs, an immunohistochemical analysis was accompanied by cytological studies thus allowing the embryonic/totipotent, meristematic/pluripotent, differentiated and callus cells to be distinguished on the basis of their phenotype. It is accepted that embryonic and meristematic cells are diverse in the phenotype (Verdeil et al., 2007), thus these features of the explant cells were used. The analysis was performed in explants before and at various time points after the induction of SE, which correlates with the previously described histological and molecular changes in Arabidopsis explants (Kurczyńska et al., 2007).

4.1. Pectic and AGP epitopes in the embryonic/totipotent cells of the Arabidopsis explants

The distribution of analyzed pectic and AGP epitopes within the

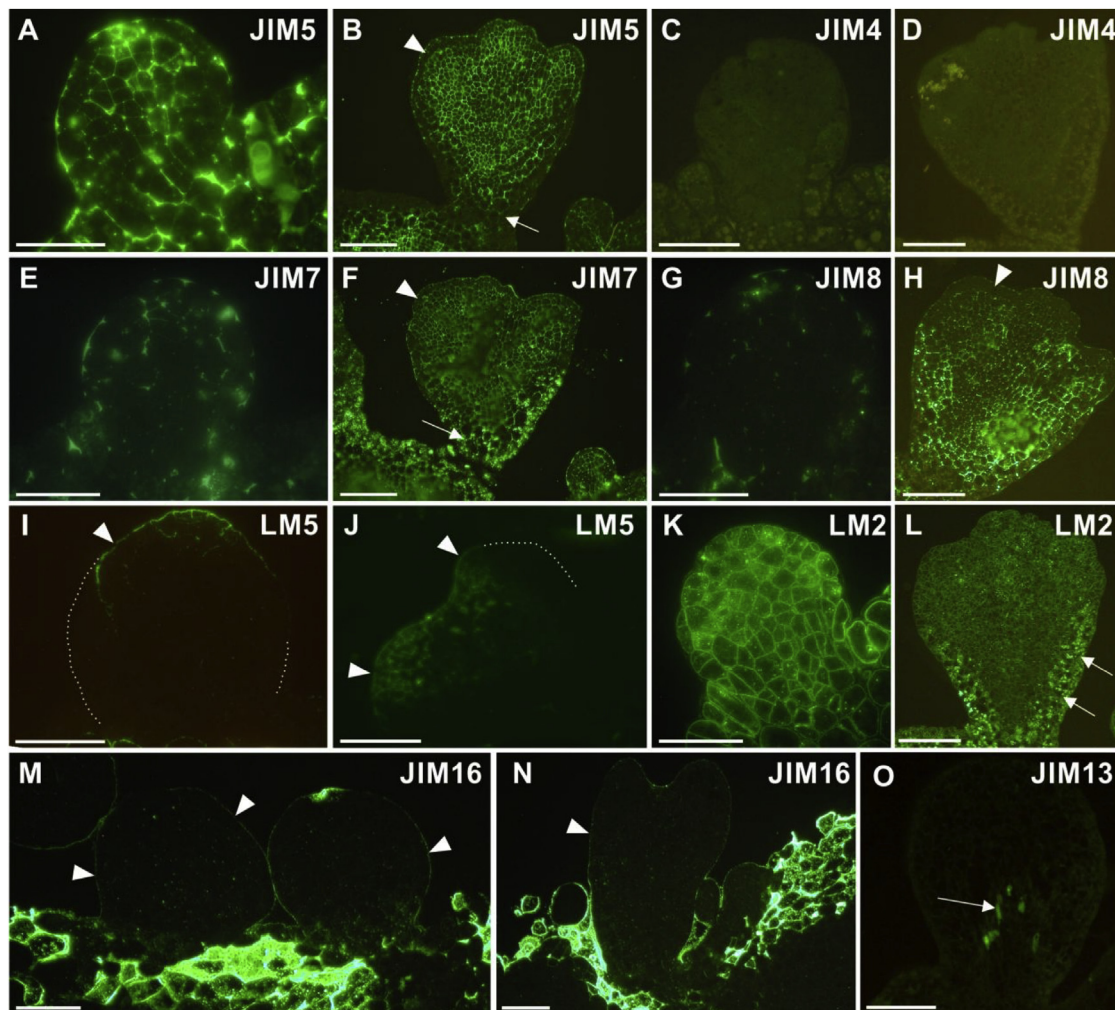


Fig. 7. Immunofluorescent detection of the pectic and AGP epitopes in somatic embryos. (A, B) The JIM5 labeling. (C, D) The JIM4 labeling. (E, F) The JIM7 labeling. (G, H) The JIM8 labeling. (I, J) The LM5 labeling. (K, L) The LM2 labeling. (M, N) The JIM16 labeling. (O) The JIM13 labeling. (A, C, E, G, I, K, M) – globular embryo/embryos; (B, D, F, H, J, L, N, O) – heart stage embryos. (B, F, H) – arrowheads indicate protodermis. (B, F, L) arrows point to basal part of embryo. (I, J) – white dotted line indicates the surface of embryo as seen in bright field. (I, J, M, N) – arrowheads indicate cells exhibiting presence of pectic epitopes. (O) – arrow indicates provascular bundle. Scale bars: (A–O) = 30 μm.

explants was spatially and temporally changed during SE. A modification of the degree of pectin methyl-esterification has been reported for other *in vitro* systems such as the androgenic embryos of *Capsicum annuum* (Bárány et al., 2010a) and the somatic embryos of *Quercus suber*

(Ramírez et al., 2004), *Citrus clementina* (Ramírez et al., 2003), *Olea europaea* (Solís et al., 2008), *Brassica napus* (Solís et al., 2016) or *Daucus carota* (Dobrowolska et al., 2012).

The most important features of embryogenic/totipotent cell

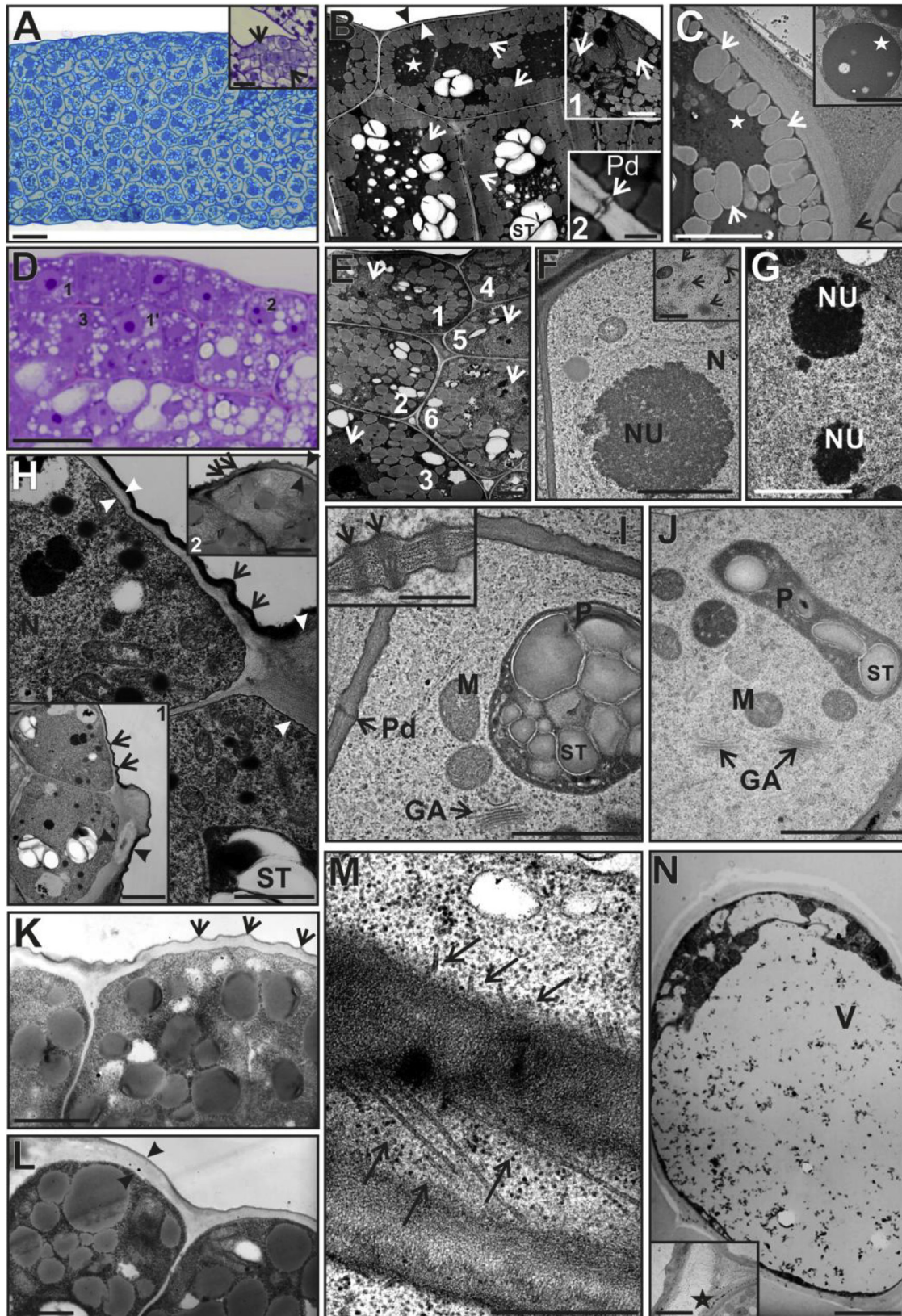
Table 3

Summarised results of immunolabeling for the globular and the heart stage somatic embryos.

Stages of embryo development	Pectins				
	JIM5	JIM7	LM5	JIM13	JIM16
Globular stage	abundant in all cells of the embryo	signal in the protodermal cells and some inner cells	signal in a few cells at the apical pole of the embryo or lack of the signal		
Heart stage	all cells apart from the basal half of the embryo	abundant in all cells, especially in the basal half of the embryo	embryo cotyledons		
Stages of embryo development	Arabinogalactan proteins				
	JIM4	JIM8	LM2	JIM13	JIM16
Globular stage	lack of the signal	pegs and inner periclinal walls of protodermal cells; apical half of the embryo	abundant presence in all cells of the embryo	lack of signal	only in the outer periclinal walls of the protoderm
Heart stage	lack of the signal	abundant presence in the ground meristem	abundant presence in the 2–3 external cell layers of the basal half of the embryo	lack of the signal	only in the outer periclinal walls of the protoderm

phenotypes (according to Verdeil et al., 2007) are a large, centrally positioned nucleus with a single prominent nucleolus, a dense cytoplasm and small vacuoles. Such a phenotype has been reported for the embryogenic cells of various plant species (for a review see

Namasivayam, 2007). At the beginning of the culture, embryogenic/totipotent cells *sensu* Verdeil et al. (2007) were not present within the explant cells. Starting at day three of the culture, the walls of the cells that were localized in the proximal parts of the cotyledons, which are



(caption on next page)

Fig. 8. Cytological and ultrastructural changes in the explant cells during the culture. General and ultrastructural view of the cytological differences between the protodermal and ground promeristem cells of the explant. (A) TBO staining; (A inset, D) PAS reaction; (B–C, E–N) TEM. (A–C) Explant in the initial stage of the culture. Pluripotent/meristematic cells were characterized by two nucleoli in the nucleus (A inset, arrows). The protodermal cells of the explant were filled with numerous oil bodies (B, C, white arrows) and protein bodies (C, C inset, asterisks) and were characterized by chloroplasts with a system of internal membranes that were not well-developed (B inset 1, arrows), the electron-dense outer layer of periclinal wall (black arrowhead) was connected with the middle lamella between the anticlinal walls (C, black arrow), electron-lucent inner layer is indicated by white arrowhead (B). Note the plasmodesmata between the explant cells (B inset 2, arrow). (D–L) Explants after 7 days of culture. (D) Cells with different phenotypes that were present in the explants, 1 and 1' – cells with a large prominent nucleolus in nucleus, 2 – cell with two nucleoli in the nucleus, 3 – cell with a nucleus without any ultrastructural changes compared to the starting point of culture. (E) Subsequent changes in the cell ultrastructure are indicated by digits (see description in Results chapter), arrows indicates nuclei. (F) A cell with a prominent nucleolus in the nucleus and abundant dictyosomes (F inset, arrows). (G) A cell with more than one nucleolus in the nucleus. (H, H inset 1 and 2) Differences in the cell wall ultrastructure appeared during the 1st week of the culture: undulated outer electron-dense layer of the protodermal wall (arrows), the thickness of the outer periclinal walls increased (indicated with two black arrowheads to mark the thickness), mainly as a result of an increase in the thickness of the inner part of the outer periclinal wall (indicated with two white arrowheads). (I, J) Changes in the cytoplasm ultrastructure in the 1st week of the culture related to the mitochondria, dictyosomes, plastids and plasmodesmata (inset, indicated with arrows). (K) Protodermal cell from the totipotent/embryogenic part of the explants with an undulated outer periclinal wall (arrows). (L) Protodermal cells from the non-embryogenic part of an explant with a thicker outer periclinal wall (two arrowheads mark the thickness). (M, N) Explant in the 2nd week of culture. Note the abundant presence of microtubules (M, arrows) in the explant cells. (N) Callus cells separated from the explant were characterized by a prominent vacuole and during the separation from explant, fibrillary material in the intercellular spaces was detected (inset, asterisk). GA – dictyosome, M – mitochondrion, N – nucleus, NU – nucleolus, P – plastid, Pd – plasmodesmata, ST – starch grain, V – vacuole. Scale bars: (A) = 20 μm , (A inset, D) = 10 μm , (B, B inset 1, B inset 2, C, E, F inset, G, H, H inset 1 & 2, I, K, L, M, N, N inset 2) = 2 μm , (D) = 10 μm , (F, F inset, N inset 1) = 1 μm , (J) = 5 μm .

embryogenic regions (for details see Kurczyńska et al., 2012), were enriched in HG with both low and high levels of esterification (recognized by the JIM5 and JIM7 antibodies, respectively), but the intensity of the JIM7 signal was much stronger, which suggests that the level of high-esterified pectin increased in the embryogenic cells. Similar results were described for the somatic embryogenesis of *Quercus alba* (Corredoira et al., 2017) and, to a lesser extent, in the embryogenic calli of *Brachypodium distachyon* (Betekhtin et al., 2016). In a banana culture, the embryogenic cells were relatively rich in the JIM5 epitope and the JIM7 epitope was less represented (Xu et al., 2011). In *Cichorium*, the immunolocalization of an epitope that is recognized by the JIM5 antibody revealed the unesterified nature of the supraembryonic network, and the highly methyl-esterified pectins that are recognized by the JIM7 antibody were only slightly present in the cell walls during the embryogenesis process (Chapman et al., 2000). In an *in vitro* culture of *Trifolium nigrescens*, low-esterified HG was most abundant during the early stages of embryo formation and a highly methyl-esterified form of HG became prevalent during embryoid maturation (Pilarska et al., 2013). The impression is that our results and those presented in the literature data are mutually exclusive, but such differences are probably the result of the analysis of slightly different stages of SE, which might be diverse in terms of the chemical composition of the cell wall. The results presented here refer only to the embryogenic/totipotent cells and the explant part where the formation of bulges has only been initiated. It is reasonable to conclude that high-esterified pectins mark embryogenic/totipotent cells in the same pattern as has been shown for other species and culture systems (Corredoira et al., 2017). Such an interpretation is consistent with our knowledge about the involvement of the methyl-esterification of HG in the postulated modification of the mechanical properties of the cell wall (Wolf et al., 2009).

Although literature data concerning the presence of the LM5 epitope in the cell walls during different developmental processes were already described (e.g. Sala et al., 2013), its distribution in cells during somatic embryogenesis has not been widely studied. The results presented here indicate that the LM5 epitope, which detects (1→4)- β -D-galactan, the side chains of RG-I, was present in some of the cells within the domain of the embryogenic cells. The diverse distribution of this epitope in the cells of the same phenotype (located in the central part of the domain and in the domain periphery) was not expected. Although the number of papers describing the contribution of this epitope in somatic embryogenesis is limited, they suggest that the LM5 epitope indicates non-embryogenic cells (Xu et al., 2011; Pilarska et al., 2013). In the above mentioned papers, cells with the LM5 epitope were characterized by a different phenotype than the one described here or they exhibited different developmental stage. Thus, we propose a hypothesis that the LM5 in the Arabidopsis explants may indicate specific cells within the

embryogenic cell clusters that are destined for embryo formation and that give rise to the pre-globular somatic embryo. If this hypothesis is correct, further studies must be performed using molecular methods.

An interesting result from that is described above is the disappearance of the JIM5 and JIM7 epitopes in the elongated cells, which according to Rocha et al. (2016) may represent one of the first signs of the acquisition of competence in this regeneration system. The acquisition of competence is the phase during which a given cell or tissue assumes a new developmental fate (Rocha et al., 2016). Thus, the disappearance of these pectic epitopes may be a marker of a competent cell within the explant.

Regarding the AGPs, we studied the distribution of the epitopes within the explants that are recognized by the JIM4, JIM8, LM2, JIM13 and JIM16 antibodies. It has been postulated that AGPs are involved in plant reproductive development (Pennell et al., 1991), pattern formation in roots (Knox et al., 1989, 1991) or maize coleoptiles (Schindler et al., 1995) and somatic embryogenesis (Pennell et al., 1991). Moreover, several other functions have been suggested such as an involvement in cell division (Serpe and Nothnagel, 1994), cell expansion (Willats and Knox, 1996) and cell death (Schindler et al., 1995).

To date, the involvement of AGPs in Arabidopsis embryogenesis has only been shown for zygotic embryos; however, in other developmental processes, including SE in other species, AGPs have been widely described (Showalter, 2001). Hu et al. (2006) and later Zhong et al. (2011) proved that AGPs are implicated in embryo germination, cotyledon formation and maintaining an undifferentiated state of the shoot meristem cells during the zygotic embryogenesis of Arabidopsis. Here, we describe the spatio-temporal changes in the occurrence of some AGP epitopes during the SE of Arabidopsis for the first time. The epitope that is recognized by the JIM4 antibody was absent in the initial explants and after several days of the culture, it appeared in cytoplasm compartments in all of the explant cells except for the provascular tissue. Literature data indicate that the JIM4 epitope may be a marker for all of the stages of the acquisition of the major tissue patterns during carrot somatic embryogenesis as it was present in the surface of proembryogenic masses (Stacey et al., 1990). The same results were obtained during maize SE (Šamaj et al., 1999a). As stated above (see results) the use of immunodetection on the light microscopy level does not allow the detection of epitopes at the ultrastructural level. The completion of such studies is an immunogold scanning electron microscopy (SEM) method which was demonstrated on the example of maize embryogenic calli and roots (Šamaj et al., 1999b). The involvement of the AGPs that are recognized by the JIM4 and JIM8 antibodies in SE was described for cultures of carrot and maize and these epitopes characterized the cells of embryogenic callus (for review see Majewska-Sawka and Nothnagel, 2000). During further studies of carrot, it was shown that the AGPs

epitope that is recognized by the JIM8 antibody is not characteristic for embryogenic cells (Toonen et al., 1997). However, cells decorated with this epitope are a source of the signal that is necessary for somatic embryo formation (McCabe et al., 1997). In indirect SE in plant cell cultures, somatic embryos develop from specialized parts of explants that are called proembryogenic masses (PEMs). Several reports have indicated that these explant areas are covered by an ECM that is composed of the JIM4, LM2, JIM16 and JIM13 epitopes (Rumyantseva, 2005). In the studies presented here, embryogenic/totipotent cells were lacking the signal that is generated by the JIM4 or JIM8 antibodies, which is comparable to the results mentioned above.

Of the group of AGP epitopes examined in this study, LM2 deserves a special comment because it gave no or a very weak signal in the cells that displayed typical embryogenic/totipotent features. However, all of the neighbouring cells were characterized by an abundant presence of this epitope in different intracellular compartments, which made the embryogenic cell clusters clearly recognized within the explant tissues. This makes LM2 a potential candidate to be a “negative” marker of embryogenic/totipotent cells in Arabidopsis explants. A similar pattern of LM2 epitope distribution was reported for the highly embryogenic cell line of a hybrid fir (Šamaj et al., 2008). In this species, the labeling was weak in the walls of the embryogenic cells and much stronger in the cytoplasm compartments of the large vacuolated suspensor cells.

It is worth adding that literature data on pectic and AGP epitopes are more abundant with respect to dicotyledonous species. Information about the proportion of individual wall components with respect to monocots are sparse, but comparison indicates that differences between monocot and dicot species exists. However, generalization based on current information requires further intensive research, especially on monocot plants (Šamaj et al., 1998; Betekhtin et al., 2018).

4.2. AGPs and pectins in the meristematic/pluripotent and differentiated cells of the Arabidopsis explants

The characteristic features of the meristematic/pluripotent cell phenotype are a prominent nucleus with two or more nucleoli and numerous small vacuoles (Verdeil et al., 2007). In our explants, the proximal part of the cotyledons swelled noticeably during the 1st week of the culture due to the cell divisions and growth that were associated with the cell wall expansion and the presence of both the JIM5 and JIM7 epitopes may be important in this process; however, these cells had no phenotype that has been described as characteristic for pluripotent/meristematic cells *sensu* Verdeil et al. (2007). A study of Bárány et al. (2010b) showed that in various developmental systems, highly esterified pectins are abundant in the walls of proliferating cells, whereas de-esterified pectins are specific markers of differentiation. Our findings agree with the above mentioned results as long as we take into account that the JIM7 epitope was abundantly present in the explant cells with a high proliferative activity.

Meristematic/pluripotent cells are similar to embryogenic/totipotent cells in terms of cytology; however, the former have a less dense cytoplasm and a smaller nucleus with one or two smaller nucleoli (Verdeil et al., 2007). Our results indicate that the LM2 epitope might function as a good marker for accurately distinguishing between totipotent and pluripotent cells, because this epitope was found abundantly in the meristematic cells and was only weakly detectable in the embryogenic cells of the explants. A similar distribution of the epitope was also reported by Konieczny et al. (2007), who observed LM2 labeling in the walls and cytoplasm of the meristematic cells of the regenerated shoot buds and leaves in a wheat anther culture. We postulate that in Arabidopsis SE, the LM2 epitope is a positive marker of meristematic/pluripotent cells.

Although the differentiated cells of the Arabidopsis explants were characterized by the presence of the majority of the epitopes that were analyzed (Table 1), the JIM4 AGP epitope appeared to be the most specific for this cell type. It was not found in the embryogenic cells or

meristematic cells, but only in some of the vacuolated cells of the proximal part of the cotyledon. Moreover, the intensity of the signal was strongly related to the level of cellular vacuolization. Thus, JIM4 labeling may indicate competent differentiated cells (Fehér, 2015) and may be the first sign of their entry into a new developmental pathway. The differentiated explant cells were also characterized by the discontinuous labeling of the cell walls with the JIM7 antibody. Such a pattern may indicate a low level of highly esterified pectins, which, according to Bárány et al. (2010a), is typical for differentiating cells.

The results from immunostaining studies presented above are confirmed by ultrastructural analyzes that have shown the diverse appearance of the outer periclinal walls and cuticle of protodermis depending on the involvement of the explant domains in the embryogenesis process and perfectly match the results described for kiwifruit (Popielarska-Konieczna et al., 2011).

4.3. Callus cells

The callus is a mass of unorganized pluripotent cells (Lee et al., 2017). In studies presented here all of the analyzed epitopes were detected in the callus cells. The differences were related to the cell wall and/or cytoplasmic localization. Because the callus is not embryogenic in the Arabidopsis system that was used in the presented studies as the development of somatic embryos from this tissue was never observed, thus the results described here characterize the non-embryogenic callus for Arabidopsis. Studies of the banana callus showed that embryogenic and non-embryogenic calli are diverse in their cell wall composition (Xu et al., 2011). The LM5 epitope was more abundant in a non-embryogenic callus compared to an embryogenic callus. The pectic epitope that is recognized by JIM5 and the AGP epitopes that were analyzed here were detected in the non-embryogenic callus of other species (Xu et al., 2011). The results presented here are in good agreement with the literature data.

4.4. Somatic embryos

The pectin composition within somatic embryos has not been widely studied, and so far, there is a lack of this information in the case of Arabidopsis somatic embryos (at least to the best of the authors' knowledge). Among the pectic epitopes that were analyzed in the presented paper, a low expression was characterized by the LM5 epitope regardless of the developmental stage of the somatic embryos. Although the JIM5 and JIM7 epitopes were abundantly present in both of the analyzed stages of the embryos, the lowest presence was detected in the protodermal cells of the embryo in later stages of development, especially for the JIM5 epitope. In the somatic embryos of *Trifolium nigrescence* Viv., the JIM7 epitope was present in the embryo body, but the signal resulting from JIM5 binding was not detected in the protodermis (Pilarska et al., 2013). Conversely, during the pollen embryogenesis of *Capsicum* (Bárány et al., 2010a) and SE of *Daucus carota* (Dobrowolska et al., 2012), the JIM7 epitope was not detected in the protodermis of the embryos. Studies on banana during SE showed that the JIM7, JIM5 and LM5 epitopes were detected in the epidermis and subepidermis and were hardly or not detected at all in the inner cells of the globular embryos (Xu et al., 2011). In older embryos, the JIM5 and LM5 epitopes were localized mainly in the cell-cell junctions of the ground meristem and the JIM7 epitope was found in the epidermal cells and ground meristem (Xu et al., 2011). Such differences in published data and the results presented here related to the pectin composition in somatic embryos probably reflect the diversity of the developmental processes in different species, but also may rely on the specific culture conditions and the source of somatic embryos.

Each of the analyzed AGP epitopes was differently located in the somatic embryos of Arabidopsis. The JIM4 epitope was not detected in any of the stages. The JIM8 epitope was hardly seen in the globular embryos but abundant in the older stage mainly in the ground

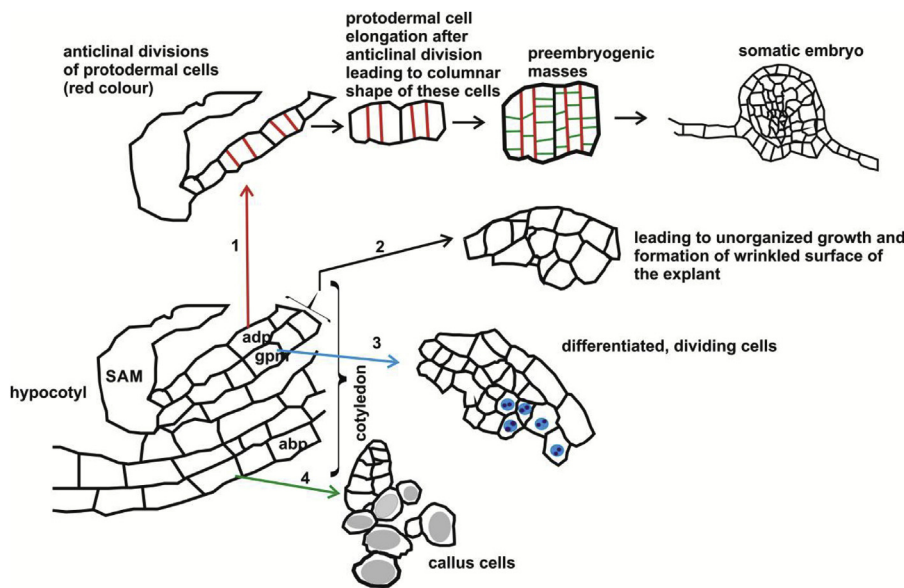


Fig. 9. The fate map of the explant cells during the SE and different pathways leading to diverse explant domains (adp, adaxial protodermis; gpm, ground promeristem; abp, abaxial protodermis; SAM, shoot apical meristem; grey color – vacuoles; blue color – nucleus with nucleoli). (For interpretation of the references to color in this figure legend, the reader is referred to the Web version of this article.)

promeristem cells. The LM2 epitope was abundantly present in all of the analyzed stages. The JIM16 epitope was present only in the outer periclinal wall of the protodermal cells, and the presence of the JIM13 epitope was very low and if it was present, accompanied the provascular bundle. Presence of JIM13 epitopes in provascular tissues is similar to described for postembryonic development (Šamaj et al., 1998), what could suggest that it is a universal marker for this tissue.

During SE of banana, it was shown that the LM2 and JIM16 epitopes were present in the globular stage embryo, but the JIM8 epitope was weakly expressed in such embryos, mainly in the embryo protodermal cells (Pan et al., 2011). For the late developmental stages of banana somatic embryos a relatively strong fluorescence was observed after immunolabeling with the LM2 and JIM16 antibodies (Pan et al., 2011). The JIM8 and JIM13 epitopes were localized solely to the tracheary elements in the vascular tissue of the very late embryos of banana, and in the later stage embryos, the JIM4 epitope was not present except for a weak signal in the epidermis (Pan et al., 2011). Thus, in the case of the JIM13 epitope, the results presented here are similar to those described above. In chicory, the AGPs that are recognized by the monoclonal antibodies LM2, JIM13 and JIM16 were localized at the outer cell walls of the epidermal cells in the globular embryos (Chapman et al., 2000). Thus, the distribution of the JIM16 epitope in Arabidopsis somatic embryos is similar to that described for chicory. In *Picea abies*, the JIM13 epitope was not detected in the early somatic embryos, and the highest expression of this epitope was found in more developed embryos (Filonova et al., 2000). Studies during microspore embryogenesis in *Brassica napus* showed that JIM8 and JIM13 binding AGPs might be involved in embryo differentiation (Tang et al., 2006). From the data presented above, it appears that some changes in the distribution of the AGPs and pectic epitopes in somatic embryos exists, and that it is species specific, but also may be influenced by the culture conditions. Despite the differences in the expression of AGPs and pectin between the somatic embryos of Arabidopsis and the somatic embryos of other species, the obtained results indicate that composition of AGPs and pectin is developmentally regulated.

5. Conclusions

In conclusion, our data show that the distribution of the selected AGP and pectic epitopes within the explants change during SE in terms of their presence in the cells that realize different developmental programs. The chemical wall composition that is described coincides with the cell phenotypes within the explants (Fig. 9). From the fate map of

the explant cells, only path 1 leads to the formation of somatic embryos. The other paths (2–4) lead to the formation of the meristematic/pluripotent cells (path 2), differentiated cells (path 3) and a non-embryogenic callus (path 4).

The findings presented here suggest that the analyzed epitopes, both pectic and AGP, are developmentally regulated. Moreover, the patterns of the occurrence of these epitopes are cell-type specific. Embryogenic cells were “positively” marked by the JIM7 and LM5 pectic epitopes and “negatively” marked by the LM2 AGP epitope. The JIM4 AGP epitope appeared to be highly specific for differentiated cells with a distinct morphology. The results presented here provide further clues into the phenomenon of the cell fate switch toward embryo development and extend the knowledge about the role of the cell wall in plant morphogenesis *in vitro*.

Because the phenotypic changes of Arabidopsis explants are described, it will be much easier and more precise to analyze the changes in gene expression during the SE using the different mutants and transgenic lines that are abundant in this species.

Author contribution

EUK, IP, KG and ID designed the research; IP established the culture and performed the immunostaining; IP, EUK, KG and ID performed the light and transmission electron microscopy analyses; IP, ID, KG and EUK analyzed the data and wrote the paper.

Acknowledgements

The research was supported financially by the Ministry of Science and Higher Education of Poland (ZFIN00000040) as a part of the statutory activities of the Department of Cell Biology, University of Silesia. Some of sections are from the MSc thesis that was realized in the Department of Cell Biology.

References

- Bárány, I., Fadón, B., Risueño, M.C., Testillano, P.S., 2010a. Cell wall components and pectin esterification levels as markers of proliferation and differentiation events during pollen development and pollen embryogenesis in *Capsicum annuum* L. J. Exp. Bot. 61, 1159–1175.
- Bárány, I., Fadón, B., Risueño, M.C., Testillano, P.S., 2010b. Microspore reprogramming to embryogenesis induces changes in cell wall and starch accumulation dynamics associated with proliferation and differentiation events. Plant Signal. Beyond Behav. 5, 341–345.
- Betekhtin, A., Rojek, M., Milewska-Hendel, A., Gawecki, R., Karcz, J., Kurczyńska, E.,

- Hasterok, R., 2016. Spatial distribution of selected chemical cell wall components in the embryogenic callus of *Brachypodium distachyon*. *PLoS One* 11, e0167426.
- Betekhtin, A., Milewska-Hendel, A., Lusinska, J., Chajec, L., Kurczyńska, E., Hasterok, R., 2018. Organ and tissue-specific localisation of selected cell wall epitopes in the zygotic embryo of *Brachypodium distachyon*. *Int. J. Mol. Sci.* 19, E725.
- Chapman, A., Blervacq, A.-S., Vasseur, J., Hilbert, J.-L., 2000. Arabinogalactan-proteins in *Cichorium* somatic embryogenesis: effect of β -glucosyl Yariv reagent and epitope localisation during embryo development. *Planta* 211, 305–314.
- Chaves, I., Regalado, A.P., Chen, M., Ricardo, C.P., Showalter, A.M., 2002. Programmed cell death induced by $(\beta$ -D-galactosyl)₃ Yariv reagent in *Nicotiana tabacum* BY-2 suspension-cultured cells. *Physiol. Plantarum* 116, 548–553.
- Clausen, M.H., Willats, W.G.T., Knox, J.P., 2003. Synthetic methyl hexagalacturonate hapten inhibitors of anti-homogalacturonan monoclonal antibodies LM7, JIM5 and JIM7. *Carbohydr. Res.* 338, 1797–1800.
- Corral-Martinez, P., Garcia-Forste, E., Bernard, S., Driouch, A., Seguí-Simarro, J.M., 2016. Ultrastructural immunolocalization of arabinogalactan protein, pectin and hemicellulose epitopes through anther development in *Brassica napus*. *Plant Cell Physiol.* 57, 2161–2174.
- Corredoira, E., Cano, V., Bárányi, I., Solís, M.-T., Rodríguez, H., Vieitez, A.-M., Rисуеño, M.C., Testillano, P.S., 2017. Initiation of leaf somatic embryogenesis involves high pectin esterification, auxin accumulation and DNA demethylation in *Quercus alba*. *J. Plant Physiol.* 213, 42–54.
- Dobrowolska, I., Kwasińska, J., Barlow, P.W., Kurczyńska, E.U., 2016. The fate of surface cell layers of *Daucus carota* (L.) embryos raised in suspension culture. *Plant Biosyst.* 150, 622–630.
- Dobrowolska, I., Majchrzak, O., Baldwin, T.C., Kurczyńska, E.U., 2012. Differences in protodermal cell wall structure in zygotic and somatic embryos of *Daucus carota* (L.) cultured on solid and in liquid media. *Protoplasma* 249, 117–129.
- Dolan, L., Linstead, P., Roberts, K., 1995. An AGP epitope distinguishes a central metaxylem initial from other vascular initials in the *Arabidopsis* root. *Protoplasma* 189, 149–155.
- Fehér, A., 2015. Somatic embryogenesis - stress-induced remodeling of plant cell fate. *BBA-Gene Regul. Mech.* 1849, 385–402.
- Fehér, A., Pasternak, T.P., Dudits, D., 2003. Transition of somatic plant cells to an embryogenic state. *Plant Cell Tissue Organ Cult.* 74, 201–228.
- Filonova, L.H., Bozhkov, P.V., Brukhin, V.B., Daniel, G., Zhivotovsky, B., von Arnold, S., 2000. Two waves of programmed cell death occur during formation and development of somatic embryos in the gymnosperm, Norway spruce. *J. Cell Sci.* 113, 4399–4411.
- Fisher, D.B., 1968. Protein staining of ribboned epon sections for light microscopy. *Histochemie* 16, 92–96.
- Fowler, M.R., Ong, L.M., Russinova, E., Atanassov, A.I., Scott, N.W., Slater, A., Elliott, M.C., 1998. Early changes in gene expression during direct somatic embryogenesis in alfalfa revealed by RAP-PCR. *J. Exp. Bot.* 49, 249–253.
- Gaj, M.D., 2001. Direct somatic embryogenesis as a rapid and efficient system for in vitro regeneration of *Arabidopsis thaliana*. *Plant Cell Tiss. Org. Cult.* 64, 39–46.
- Gaj, M.D., Zhang, S.B., Harada, J.J., Lemaux, P.G., 2005. Leafy cotyledon genes are essential for induction of somatic embryogenesis of *Arabidopsis*. *Planta* 222, 977–988.
- Gamborg, O.L., Miller, R.A., Ojima, K., 1968. Nutrient requirements of suspension cultures of soybean root cells. *Exp. Cell Res.* 50, 151–158.
- Hu, Y., Qin, Y., Zhao, J., 2006. Localization of an arabinogalactan protein epitope and the effects of Yariv phenylglycoside during zygotic embryo development of *Arabidopsis thaliana*. *Protoplasma* 229, 21–31.
- Ikeuchi, M., Sugimoto, K., Iwase, A., 2013. Plant callus: mechanisms of induction and repression. *Plant Cell* 25, 3159–3173.
- Jones, L., Seymour, G.B., Knox, J.P., 1997. Localization of pectic galactan in tomato cell walls using a monoclonal antibody specific to (1→4)- β -D-galactan. *Plant Physiol. (Wash. D C)* 113, 1405–1412.
- Kikuchi, A., Satoh, S., Nakamura, N., Fujii, T., 1995. Differences in pectic polysaccharides between carrot embryogenic and non-embryogenic calli. *Plant Cell Rep.* 14, 279–284.
- Knox, J.P., 1992. Cell-adhesion, cell-separation and plant morphogenesis. *Plant J.* 2, 137–141.
- Knox, J.P., Day, S., Roberts, K., 1989. A set of cell-surface glycoproteins forms an early marker of cell position, but not cell type, in the root apical meristem of *Daucus carota* L. *Development* 106, 47–56.
- Knox, J.P., Linstead, P.J., Peart, J., Cooper, C., Roberts, K., 1991. Developmentally regulated epitopes of cell surface arabinogalactan proteins and their relation to root tissue pattern formation. *Plant J.* 1, 317–326.
- Konieczny, R., Świerczyńska, J., Czapllicki, A.Z., Bohdanowicz, J., 2007. Distribution of pectin and arabinogalactan protein epitopes during organogenesis from androgenic callus of wheat. *Plant Cell Rep.* 26, 355–363.
- Kurczyńska, E.U., Gaj, M.D., Ujczak, A., Mazur, E., 2007. Histological analysis of direct somatic embryogenesis in *Arabidopsis thaliana* (L.) Heynh. *Planta* 226, 619–628.
- Kurczyńska, E.U., Potocka, I., Dobrowolska, I., Kulinska-Lukaszek, K., Sala, K., Wrobel, J., 2012. Cellular markers for somatic embryogenesis. In: Ken-ichi, S. (Ed.), *Embryogenesis*. InTech, Rijeka, pp. 307–332.
- Langan, K.J., Nothnagel, E.A., 1997. Cell surface arabinogalactan-proteins and their relation to cell proliferation and viability. *Protoplasma* 196, 87–98.
- Lee, K., Park, O.S., Seo, P.J., 2017. *Arabidopsis* ATXR2 deposits H3K36me3 at the promoters of *LBD* genes to facilitate cellular dedifferentiation. *Sci. Signal.* 10, eaan0316.
- Magioli, C., Barróco, R.M., Rocha, C.A.B., de Santiago-Fernandes, L.D., Mansur, E., Engler, G., Margis-Pinheiro, M., Sabetto-Martins, G., 2001. Somatic embryo formation in *Arabidopsis* and eggplant is associated with expression of a glycine-rich protein gene (*Atgrp-5*). *Plant Sci.* 161, 559–567.
- Majewska-Sawka, A., Nothnagel, E.A., 2000. The multiple roles of arabinogalactan proteins in plant development. *Plant Physiol. (Wash. D C)* 122, 3–9.
- McCabe, P.F., Valentine, T.A., Forsberg, L.S., Pennell, R.I., 1997. Soluble signals from cells identified at the cell wall establish a developmental pathway in carrot. *Plant Cell* 9, 2225–2241.
- Milewska-Hendel, A., Baczevska, A.H., Sala, K., Dmuchowski, W., Brągoszewska, P., Gozdowski, D., Jozwiak, A., Chojnacki, T., Swiezewska, E., Kurczyńska, E.U., 2017. Quantitative and qualitative characteristics of cell wall components and prenyl lipids in the leaves of *Tilia x euchlora* trees growing under salt stress. *PLoS One* 12, e0172682.
- Mozgová, I., Muñoz-Viana, R., Hennig, L., 2017. PRC2 represses hormone-induced somatic embryogenesis in vegetative tissue of *Arabidopsis thaliana*. *PLoS Genet.* 13, e1006562.
- Namasivayam, P., 2007. Acquisition of embryogenic competence during somatic embryogenesis. *Plant Cell Tissue Organ Cult.* 90, 1–8.
- Namasivayam, P., Skepper, J., Hanke, D., 2006. Identification of a potential structural marker for embryogenic competency in the *Brassica napus* spp. *oleifera* embryogenic tissue. *Plant Cell Rep.* 25, 887–895.
- Pan, X., Yang, X., Lin, G., Zou, R., Chen, H., Šamaj, J., Xu, C., 2011. Ultrastructural changes and the distribution of arabinogalactan proteins during somatic embryogenesis of banana (*Musa* spp. AAA cv. 'Yueyoukang 1'). *Physiol. Plantarum* 142, 372–389.
- Pennell, R.I., Janniche, L., Kjellbom, P., Scofield, G.N., Peart, J., Roberts, K., 1991. Developmental regulation of a plasma-membrane arabinogalactan protein epitope in oilseed rape flowers. *Plant Cell* 3, 1317–1326.
- Pielach, A., Leroux, O., Domozych, D.S., Knox, J.P., Popper, Z.A., 2014. Arabinogalactan protein-rich cell walls, paramural deposits and ergastic globules define the hyaline bodies of rhinanthoid Orobanchaceae haustoria. *Ann. Bot.* 114, 1359–1373.
- Pilarska, M., Knox, J.P., Konieczny, R., 2013. Arabinogalactan-protein and pectin epitopes in relation to an extracellular matrix surface network and somatic embryogenesis and callogenesis in *Trifolium nigrescens* Viv. *Plant Cell Tissue Organ Cult.* 115, 35–44.
- Popielarska-Konieczna, M., Kozieradzka-Kiszkurno, M., Bohdanowicz, J., 2011. Cutin plays a role in differentiation of endosperm-derived callus of kiwifruit. *Plant Cell Rep.* 30, 2143–2152.
- Potocka, I., Baldwin, T.C., Kurczyńska, E.U., 2012. Distribution of lipid transfer protein 1 (LTP1) epitopes associated with morphogenic events during somatic embryogenesis of *Arabidopsis thaliana*. *Plant Cell Rep.* 31, 2031–2045.
- Qin, Y., Zhao, J., 2006. Localization of arabinogalactan proteins in egg cells, zygotes, and two-celled proembryos and effects of β -D-glucosyl Yariv reagent on egg cell fertilization and zygote division in *Nicotiana tabacum* L. *J. Exp. Bot.* 57, 2061–2074.
- Rajesh, M.K., Fayas, T.P., Naganeswaran, S., Rachana, K.E., Bhavyashree, U., Sajini, K.K., Karun, A., 2016. De novo assembly and characterization of global transcriptome of coconut palm (*Cocos nucifera* L.) embryogenic calli using Illumina paired-end sequencing. *Protoplasma* 253, 913–928.
- Ramírez, C., Chiancone, B., Testillano, P.S., García-Fojeda, B., Germaná, M.-A., Rисуеño, M.-C., 2003. First embryogenic stages of *Citrus* microspore-derived embryos. *Acta Biol. Cracov. Bot.* 45, 53–58.
- Ramírez, C., Testillano, P.S., Pintos, B., Moreno-Risueño, M.A., Bueno, M.A., Rисуеño, M.-C., 2004. Changes in pectins and MAPKs related to cell development during early microspore embryogenesis in *Quercus suber* L. *Eur. J. Cell Biol.* 83, 213–225.
- Rocha, D.I., Pinto, D.L.P., Vieira, L.M., Tanaka, F.A.O., Dornelas, M.C., Otoni, W.C., 2016. Cellular and molecular changes associated with competence acquisition during passion fruit somatic embryogenesis: ultrastructural characterization and analysis of *SERK* gene expression. *Protoplasma* 253, 595–609.
- Rodríguez-Sanz, H., Manzanera, J.-A., Solís, M.-T., Gómez-Garay, A., Pintos, B., Rисуеño, M.C., Testillano, P.S., 2014. Early markers are present in both embryogenesis pathways from microspores and immature zygotic embryos in cork oak, *Quercus suber* L. *BMC Plant Biol.* 14, 224.
- Rosas, M.M., Quiroz-Figueroa, F., Shannon, L.M., Ruiz-May, E., 2016. The current status of proteomic studies in somatic embryogenesis. In: Loyola-Vargas, V.M., Ochoa-Alejo, N. (Eds.), *Somatic Embryogenesis: Fundamental Aspects and Applications*. Springer International Publishing, Switzerland, pp. 103–119.
- Rumyantseva, N.I., 2005. Arabinogalactan proteins: involvement in plant growth and morphogenesis. *Biochemist* 70, 1073–1085.
- Rumyantseva, N.I., Šamaj, J., Ensikat, H.-J., Sal'nikov, V.V., Kostyukova, Y.A., Baluška, F., Volkman, D., 2003. Changes in the extracellular matrix surface network during cyclic reproduction of proembryonic cell complexes in the *Fagopyrum tataricum* (L.) Gaertn. callus. *Dokl. Biol. Sci.* 391, 375–378.
- Sala, K., Potocka, I., Kurczyńska, E., 2013. Spatio-temporal distribution and methyl-esterification of pectic epitopes provide evidence of developmental regulation of pectins during somatic embryogenesis in *Arabidopsis thaliana*. *Biol. Plantarum* 57, 410–416.
- Šamaj, J., Baluška, F., Volkman, D., 1998. Cell-specific expression of two arabinogalactan protein epitopes recognized by monoclonal antibodies JIM8 and JIM13 in maize roots. *Protoplasma* 204, 1–12.
- Šamaj, J., Baluška, F., Bobák, M., Volkman, D., 1999a. Extracellular matrix surface network of embryogenic units of friable maize callus contains arabinogalactan-proteins recognized by monoclonal antibody JIM4. *Plant Cell Rep.* 18, 369–374.
- Šamaj, J., Ensikat, H.-J., Baluška, F., Knox, J.P., Barthlott, W., Volkman, D., 1999b. Immunogold localization of plant surface arabinogalactan-proteins using glycerol liquid substitution and scanning electron microscopy. *J. Microsc.* 193, 150–157.
- Šamaj, J., Salaj, T., Matúšová, R., Salaj, J., Takáč, T., Šamajová, O., Volkman, D., 2008. Arabinogalactan-protein epitope Gal4 is differentially regulated and localized in cell lines of hybrid fir (*Abies alba* × *Abies cephalonica*) with different embryogenic and regeneration potential. *Plant Cell Rep.* 27, 221–229.
- Schindler, T., Bergfeld, R., Schopfer, P., 1995. Arabinogalactan proteins in maize coleoptiles: developmental relationship to cell death during xylem differentiation but not to extension growth. *Plant J.* 7, 25–36.

- Schultz, C., Gilson, P., Oxley, D., Youl, J., Bacic, A., 1998. GPI-anchors on arabinogalactan-proteins: implications for signalling in plants. *Trends Plant Sci.* 3, 426–431.
- Seifert, G.J., Roberts, K., 2007. The biology of arabinogalactan proteins. *Annu. Rev. Plant Biol.* 58, 137–161.
- Serpe, M.D., Nothnagel, E.A., 1994. Effects of Yariv phenylglycosides on *Rosa* cell suspensions: evidence for the involvement of arabinogalactan-proteins in cell proliferation. *Planta* 193, 542–550.
- Showalter, A.M., 2001. Arabinogalactan-proteins: structure, expression and function. *Cell. Mol. Life Sci.* 58, 1399–1417.
- Smallwood, M., Yates, E.A., Willats, W.G.T., Martin, H., Knox, J.P., 1996. Immunochemical comparison of membrane-associated and secreted arabinogalactan-proteins in rice and carrot. *Planta* 198, 452–459.
- Smertenko, A., Bozhkov, P.V., 2014. Somatic embryogenesis: life and death processes during apical-basal patterning. *J. Exp. Bot.* 65, 1343–1360.
- Solíis, M.-T., Berenguer, E., Risueño, M.C., Testillano, P.S., 2016. BnPME is progressively induced after microspore reprogramming to embryogenesis, correlating with pectin de-esterification and cell differentiation in *Brassica napus*. *BMC Plant Biol.* 16, 176.
- Solíis, M.-T., Pintos, B., Prado, M.-J., Bueno, M.-A., Raska, I., Risueño, M.-C., Testillano, P.S., 2008. Early markers of *in vitro* microspore reprogramming to embryogenesis in olive (*Olea europaea* L.). *Plant Sci.* 174, 597–605.
- Stacey, N.J., Roberts, K., Knox, J.P., 1990. Patterns of expression of the JIM4 arabinogalactan-protein epitope in cell cultures and during somatic embryogenesis in *Daucus carota* L. *Planta* 180, 285–292.
- Tang, F., Hajkova, P., Barton, S.C., Lao, K., Surani, M.A., 2006. MicroRNA expression profiling of single whole embryonic stem cells. *Nucleic Acids Res.* 34, e9.
- Thompson, H.J.M., Knox, J.P., 1998. Stage-specific responses of embryogenic carrot cell suspension cultures to arabinogalactan protein-binding β -glucosyl Yariv reagent. *Planta* 205, 32–38.
- Toonen, M.A.J., Schmidt, E.D.L., van Kammen, A., de Vries, S.C., 1997. Promotive and inhibitory effects of diverse arabinogalactan proteins on *Daucus carota* L. somatic embryogenesis. *Planta* 203, 188–195.
- Verdeil, J.-L., Alemanno, L., Niemenak, N., Tranbarger, T.J., 2007. Pluripotent versus totipotent plant stem cells: dependence versus autonomy? *Trends Plant Sci.* 12, 245–252.
- Willats, W.G.T., Knox, J.P., 1996. A role for arabinogalactan-proteins in plant cell expansion: evidence from studies on the interaction of β -glucosyl Yariv reagent with seedlings of *Arabidopsis thaliana*. *Plant J.* 9, 919–925.
- Willats, W.G.T., McCartney, L., Mackie, W., Knox, J.P., 2001. Pectin: cell biology and prospects for functional analysis. *Plant Mol. Biol.* 47, 9–27.
- Wójcikowska, B., Gaj, M.D., 2017. Expression profiling of *AUXIN RESPONSE FACTOR* genes during somatic embryogenesis induction in *Arabidopsis*. *Plant Cell Rep.* 36, 843–858.
- Wolf, S., Mouille, G., Pelloux, J., 2009. Homogalacturonan methyl-esterification and plant development. *Mol. Plant* 2, 851–860.
- Xu, C., Zhao, L., Pan, X., Šamaj, J., 2011. Developmental localization and methylesterification of pectin epitopes during somatic embryogenesis of banana (*Musa* spp. AAA). *PLoS One* 6, e22992.
- Yates, E.A., Valdor, J.-F., Haslam, S.M., Morris, H.R., Dell, A., Mackie, W., Knox, J.P., 1996. Characterization of carbohydrate structural features recognized by anti-arabinogalactan-protein monoclonal antibodies. *Glycobiology* 6, 131–139.
- Zhong, J., Ren, Y.J., Yu, M., Ma, T.F., Zhang, X.L., Zhao, J., 2011. Roles of arabinogalactan proteins in cotyledon formation and cell wall deposition during embryo development of *Arabidopsis*. *Protoplasma* 248, 551–563.